Ultrasound in Med. & Biol., Vol. 41, No. 4, pp. 905–928, 2015

0301-5629/$ - see front matter

http://dx.doi.org/10.1016/j.ultrasmedbio.2014.11.019

● *Review*

A REVIEW OF LOW-INTENSITY ULTRASOUND FOR CANCER THERAPY

ANDREW K. W. WOOD* and CHANDRA M. SEHGAL†

*Department Clinical Studies, School of Veterinary Medicine, University of Pennsylvania, Philadelphia, Pennsylvania, USA; and †Department of Radiology, School of Medicine, University of Pennsylvania, Philadelphia, Pennsylvania, USA

(*Received* 14 *March* 2014; *revised* 13 *November* 2014; *in final form* 24 *November* 2014)

Abstract—The literature describing the use of low-intensity ultrasound in four major areas of cancer therapy—sonodynamic therapy, ultrasound-mediated chemotherapy, ultrasound-mediated gene delivery and anti-vascular ultrasound therapy—was reviewed. Each technique consistently resulted in the death of cancer cells, and the bio-effects of ultrasound were attributed primarily to thermal actions and inertial cavitation. In each therapeutic modality, theranostic contrast agents composed of microbubbles played a role in both therapy and vascular imaging. The development of these agents is important as it establishes a therapeutic–diagnostic platform that can monitor the success of anti-cancer therapy. Little attention, however, has been given either to the direct assessment of the mechanisms underlying the observed bio-effects or to the viability of these therapies in naturally occurring cancers in larger mammals; if such investigations provided encouraging data, there could be prompt application of a therapy technique in the treatment of cancer patients. (E-mail: Sehgalc@uphs.upenn.edu) © **2015 World Federation for Ultrasound in Medicine & Biology.**

Key Words: **Low-intensity ultrasound, Cancer therapy, Sonodynamic therapy, Ultrasound-mediated chemotherapy, Anti-vascular ultrasound, Ultrasound bio-effects, Microbubble contrast agent.**

INTRODUCTION

Low-intensity ultrasound has been used in a variety of therapeutic applications. Together with sensitizing molecules it has been used to affect cancer cells (sonodynamic therapy); it has enhanced the activity of chemotherapeutic molecules in cancer therapy (ultrasound-mediated chemotherapy); it has been used to affect cells and their components directly (sonoporation); it has been used for gene delivery or transfection and to promote bone and tissue heating/healing and for its anti-vascular actions on tumor neovasculature. This appraisal of the literature focuses on the role of low-intensity ultrasound in cancer therapy. The published studies have included *in vitro* observations of cancer cell suspensions and cultures and the treatment of an extensive range of implanted tumors in small laboratory animals. This review covers four of the major areas in which low-intensity ultrasound has been used for cancer therapy studies: sonodynamic therapy, ultrasound-mediated chemotherapy, ultrasound-mediated gene delivery and anti-vascular ultrasound therapy.

Address correspondence to: Chandra M. Sehgal, PhD, Professor, Department of Radiology, University of Pennsylvania Medical Center, 3400 Spruce Street, Philadelphia, PA 19104, USA. E-mail: Sehgalc@uphs.upenn.edu

To date there is no widely accepted definition of low-intensity ultrasound, but this review has centered on investigations in which cancer cells or tumors have generally been insonated with an intensity less than 5.0 W cm^{-2}, corresponding to a root-mean-square pressure amplitude of about 0.3 MPa. Many variable sonication conditions have been used for the studies in the literature, making it difficult to make accurate comparisons between the reports. To aid the comparisons in this review, pressure–intensity conversions were made using the formula $I = p^2/\rho c$, where I = intensity, p = root mean square pressure amplitude, ρ = density and c = sound speed (Preston 1991).

In general terms, insonation of neoplasms with low-intensity ultrasound is easy to perform as it does not require a focused beam (that must be accurately located), the apparatus is relatively inexpensive, the bio-effects in adjacent normal tissues are commonly believed to be minimal and it is possible to easily target sensitizing or chemotherapeutic molecules and microbubbles located within the lumens of the tumor neovasculature. Treatment times are, however, prolonged in comparison to those used in high-intensity focused ultrasound, but repeated treatments or dose fractionation is easily performed.

SONODYNAMIC THERAPY

The term *sonodynamic therapy* derives from photodynamic therapy. However, unlike photodynamic therapy, in which photosensitizers are excited directly by light to produce reactive oxygen species, sonodynamic therapy is mediated via ultrasound-induced cavitation and sonosensitizers to produce free radicals that kill nearby rapidly dividing cancer cells (Fig. 1). An attraction of sonodynamic therapy, in which continuous, low-intensity ultrasound at diagnostic ultrasound frequencies is used, is its ability to treat deeply located tumors. On the other hand, photodynamic therapy uses visible light, which attenuates rapidly in tissues, has limited penetration and can be employed only superficially or intraoperatively. When comparing the efficacy of the two methods, Jin et al. (2000) treated a subcutaneously located murine squamous cell carcinoma and found that sonodynamic therapy inhibited tumor growth by 77%, compared with 27% for photodynamic therapy. The latter was not as effective a therapy in the deeper regions of the tumor.

Sonodynamic therapy initially used the same light-sensitive agents, hematoporphyrin and its derivatives, that had been developed for photodynamic therapy. An ideal sensitizing agent should be preferentially taken up and retained in the tumor so that the therapy damages cancer cells, but has minimal bio-effects in the surrounding normal tissues; the agent should also be relatively non-toxic to normal mammalian tissues. To improve the efficacy of treating solid tumors, it is important that the sonosensitizer is injected intravenously before insonation, rather than directly into the tumor, so that it is more fully and evenly distributed throughout the neoplasm (Ninomiya et al. 2012).

Overviews of the sonosensitizers used in the therapy have been published (Chen et al. 2014; Feril et al. 2011; Kuroki et al. 2007; Shibaguchi et al. 2011). In sonodynamic therapy, the sonication parameters (usually 1.0–2.0 MHz at an intensity of 0.5 to 3.0 W cm^{-2}) (Tables 1 and 2) have been selected to produce inertial cavitation in a cell culture or tumor, where microbubbles rapidly collapse resulting in shockwaves that produce free radicals and a cascade of molecular events that activate the sonosensitizer and, in turn, damage the cancer cells (Misik and Riesz 2000; Rosenthal et al. 2004; Yu et al. 2004c). Although the production of reactive oxygen species appears important in the anti-tumor affect, Wang et al. (2011a) stated that thermal effects cannot be excluded. In addition to these direct cytotoxic effects on neoplastic cells, it is also important to consider other possible effects on the growing tumor, including its vascular supply. Gao et al. (2013) reported that sonodynamic therapy also has an anti-vascular effect and inhibits tumor neovascularization. Another approach has been to use a chemotherapeutic agent as the sonosensitizer. In *in vitro* studies of adriamycin (Gao et al. 2010), cisplatin (Bernard et al. 2011, 2012 [0.4 ± 0.02 MPa]) and doxorubicin (Liang et al. 2013), it was found that these agents were cytostatic, and apoptosis was further enhanced when they were used in combination with chlorine e6 (Gao et al. 2010) or a hematoporphyrin (Liang et al. 2013).

After the initial descriptions of sonodynamic therapy by Yumita et al. (1989) and Umemura et al. (1990), there were numerous confirming reports that further revealed the bio-effects of the therapy. In contrast to the earlier reviews, we have grouped the research studies according to the type of cancer cell and accompanying sonosensitizer that were insonated; the aim was to provide a guide to previous sonodynamic studies in which the type of cancer receiving therapy is emphasized (Tables 1 and 2). Considerable data have been published over the past 25 y using many different sonosensitizers and involving many types of cancer (Tables 1 and 2), and each report has consistently indicated the significant bio-effects of sonodynamic therapy. The relative merits of each of these numerous sonodynamic agents are, however, difficult to determine as each of the agents was investigated in isolation without comparing the efficacy of one against another. Thus, key questions remain to be answered, for example: Are the recently developed nanoparticle sonosensitizers any more effective than the original porphyrins in killing cancer cells?

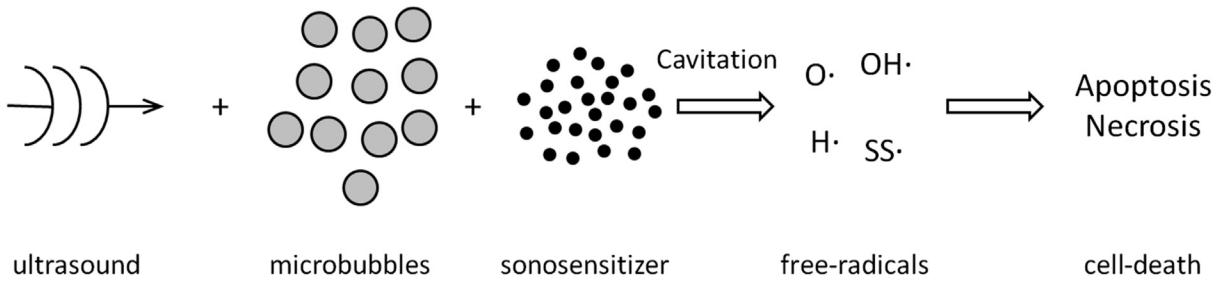

Fig. 1. Schema of sonodynamic therapy. Low-intensity insonation of cancer cells in the presence of a sonosensitizer causes cavitation, leading to the production of free radicals with resultant cell death by apoptosis and necrosis.

Table 1. Sonodynamic therapy of cell cultures and suspensions

Cancer cell culture/suspension	Sonosensitizer	Insonation parameters		Reference
		MHz	W cm^{-2}	
i. Murine sarcoma 180	Hematoporphyrin	1.92	1.27–3.18	Yumita et al. 1989
	Hematoporphyrin	1.9	1.8	Umemura et al. 1990
	Hematoporphyrin	1.75	1.4	Tang et al. 2008a, 2008b
	Hematoporphyrin	1.8	2.1	Tang et al. 2008c
	Hematoporphyrin	1.6	1.0–6.0	Wang et al. 2008a
	Pheobromide-a	1.92	4.5	Umemura et al. 1996a
	ATX-S10	1.92	4.5	Yumita et al. 2000a
	Photofrin II	1.93	5.9	Yumita et al. 2000c
	Protoporphyrin IX	1.0	5.0	Umemura et al. 1996b
	Protoporphyrin IX	2.2	1.0–7.0	Liu et al. 2006a
	Protoporphyrin IX	2.2	3.0	Wang et al. 2008c
	Protoporphyrin IX	2.2	3.0	Wang et al. 2008b
	Protoporphyrin IX	1.1	0.64–2.1	Wang et al. 2010
	Rose Bengal derivative	1.92	2.0–8.0	Sugita et al. 2010
	DCPH–P–Na(I)	2.0	5.9	Yumita et al. 2010
	NPe6	1.92	4.5	Yumita et al. 2011
	Polyhydroxy fullerenes	1.92	4.5	Yumita et al. 2013
ii. Hepatic	Hematoporphyrin	1.92	1.27–3.18	Yumita et al. 1989
	Hematoporphyrin	1.43	1.0–4.0	Liu et al. 2008b
	Titanium nanoparticles	1.0	0.1	Ninomiya et al. 2012
	Titanium nanoparticles	0.5, 1.0	0.8, 0.4	Ninomiya et al. 2014
	Hypocrellin-B	1.7	0.46	Wang et al. 2012b
iii. Nasopharyngeal	Curcumin	1.7	0.46	Wang et al. 2011b
	Curcumin	1.7	0.46	Wang et al. 2011c
	Curcumin	1.7	0.46	Wang et al. 2012c
iv. Glioma	$ZnPcS_2$ P_2	1.0	0.5	Chen et al. 2012b
	HMME	1.0	0.5	Li et al. 2013
	Photofrin	1.0	0.5	Xu et al. 2012
	Photofrin	1.0	0.5	Xu et al. 2013
	Titanium nanoparticles	1.0	1.0	Yamaguchi et al. 2011b
v. Human breast	Protoporphyrin IX	1.1	1.0	Li et al. 2012b
	Chlorin e6	1.0	0.36, 0.72	Wang et al. 2013b
	Chlorin e6 + adriamycin	1.0	0.5–2.0	Gao et al. 2010
vi. Ovarian	Cisplatin	1.0	2.0	Bernard et al. 2011
	Methylene blue	1.7	0.46	Xiang et al. 2011
vii. Other				
Acute myeloid leukemia	Chlorine e6	1.1	1.0	Su et al. 2013b
Cholangiocarcinoma	Hematoporphyrin + doxorubicin	1.2	0.5–2.0	Liang et al. 2013
Ehrlich ascites	Protoporphyrin IX	1.34	1.0-5.0	Zhao et al. 2009
Gastric	Antibody/porphyrin	1.0	1.0	Abe et al. 2002
Human leukemia	Protoporphyrin IX	1.1	1.0	Su et al. 2014
Human melanoma	Cisplatin	1.0	1.0	Bernard et al. 2012
Histiocytic lymphoma	Hematoporphyrin	1.1	1.0	Su et al. 2013a
Murine leukemia	Protoporphyrin IX	1.1	0.64–2.1	Wang et al. 2013c
Murine mammary	Chlorine e6	1.0	0.36, 0.72	Li et al. 2013
Tongue	5-Aminolevulinic acid	1.0	0.6, 0.8	Lv et al. 2012
Multiple cell lines	Porphyrin derivative	1.0	1.0	Tsuru et al. 2012
		1.0	0.5–2.0	Hachimine et al. 2007
viii. Non-neoplastic (endothelial cells)	5-Aminolevulinic acid	1.0	1.0	Gao et al. 2013

ATX-S10 = 4-formyloximethylidene-3-hydroxy-2-vinyl-deuterio-porphynyl(IX)-6,7-diaspartic acid; DCPH–P–Na(I) = 13,17-bis(1-carboxyethyl)-8-[2-(2,4-dichlorophenyl-hydrazono)ethylidene]-3-ethenyl-7-hydroxy-2,7,12,18-tetramethylchlorin; Pe6 = mono-l-aspartyl chlorin e6; HMME = hematoporphyrin monomethyl ether.

Sonodynamic therapy has routinely caused apoptosis in cancer cell suspensions and cultures and inhibited tumor growth in animal models of cancer. The therapy's effectiveness has also been reported in more deeply located tumors, including those of the central nervous system (Gao et al. 2013; Jeong et al. 2012; Ohmura et al. 2011). Post-therapy histologic studies have consistently indicated damage to the ultrastructure of the cancer cells, including destruction of cell membranes, mitochondrial swelling and chromatin condensation (Liu et al. 2006a, 2007a, 2007b, 2008a; Wang et al. 2008a, 2011c, 2012c); it was considered that these changes induced by the therapy may have mediated cancer cell death. Combining photodynamic therapy with sonodynamic therapy had a synergistic effect in solid tumors with additional post-therapy tumor necrosis, inhibition of tumor growth and increased survival times (Jin et al. 2000; Tserkovsky et al. 2012).

Table 2. Sonodynamic therapy of tumors*

Tumor	Sonosensitizer	Insonation parameter		Reference
		MHz	W cm^{-2}	
i. Murine sarcoma 180	Hematoporphyrin	1.92	1.7	Yumita et al. 1990
	Pheobromide-a	1.92	3.0	Umemura et al. 1996a
	Protoporphyrin IX	2.2	5.0	Liu et al. 2007a, 2007b
	Sinoporphyrin sodium	1.9	2.0–6.0	Li et al. 2013
ii. Colon	ATX-S10	2.0	3.0	Yumita et al. 2000a
	Photofrin II	1.92	1.0–5.0	Yumita et al. 2000b
	Protoporphyrin IX/nanoparticles	1.1	2.0	Sazgarnia et al. 2011
	Protoporphyrin IX/nanoparticles	1.1	2.0	Shanei et al. 2012
	NPe6	2.0	3.0	Yumita et al. 2011
	Polyhydroxy fullerenes	2.0	3.0	Yumita et al. 2013
iii. Hepatic	Hematoporphyrin	1.43	2.0	Liu et al. 2008b
	Protoporphyrin IX	1.43	3.0	Wang et al. 2011a
	Titanium oxide nanoparticles	1.0	1.0	Ninomiya et al. 2012
	Hematoporphyrin microbubbles	1.0	2.0	Zheng et al. 2012
	Chlorin e6	1.56	4.0	Shi et al. 2011
iv. Glioma (rats)	5-Aminolevulinic acid	1.04	10.0	Ohmura et al. 2011
	5-Aminolevulinic acid	1.0	2.65	Jeong et al. 2012
	Chlorin e6/polyvinyl pyrrolidone	1.0	0.4–1.0	Tserkovsky et al. 2012
v. Breast	Photofrin	0.015/1.0	0.2, 2.0	Barati and Mokhtari-Dizaji 2010
	No sensitizer	0.015/1.0	0.2, 2.0	Barati et al. 2009
vi. Gastric	Antibody/gallium–porphyrin	1.0	2.0	Abe et al. 2002
	Porphyrin derivative	1.0	2.0	Tsuru et al. 2012
vii. Other Squamous cell	Gallium–porphyrin/pheophorbide-a	1.0	0.51	Jin et al. 2000
Osteosarcoma (rats)	Hematoporphyrin	10.5	0.8	Tian et al. 2009
Small cell lung	Chlorin e6	1.0	0.4–1.6	Chen et al. 2013a
Tongue	5-Aminolevulinic acid	1.1	2.0	Gao et al. 2013
Human MKN-45	DCPH–P–Na(I)	1.0	2.0	Hachimine et al. 2007

ATX-S10 = 4-formyloximethylidene-3-hydroxy-2-vinyl-deuterio-porphynyl(IX)-6,7-diaspartic acid; NPe6 = mono-l-aspartyl chlorin e6.
* Unless otherwise stated all tumors were in mice.

As many of the intravenously injected sonosensitizers (Tables 1 and 2) were initially developed for use in photodynamic therapy, it is important that those used in the future for sonodynamic therapy should have low or no sensitivity to light and cause minimal cutaneous side effects (Gao et al. 2013; Ninomiya et al. 2012; Shibaguchi et al. 2011; Tsuru et al. 2012). Preliminary data from solid tumors support the administration of a regimen of multiple therapies to further enhance the bio-effects and so reduce tumor growth and size; fractionation will also reduce the thermal effects of therapy (Jeong et al. 2012).

Combination of the sonosensitizer with a microbubble contrast agent may lead to important future developments in sonodynamic therapy (Zheng et al. 2012). The combined agent can then be classified as a theranostic agent as the entry of the loaded microbubbles into the tumor vasculature can be monitored by ultrasound imaging, and once it is detected within the tumor by diagnostic ultrasound, sonodynamic therapy can be initiated. A therapeutic–diagnostic platform is established that can monitor the efficacy of therapy (Lionetti and Paddeu 2010). Further, insonation of the microbubble may lead to additional significant local thermal bio-effects with destruction of the endothelial cells lining the tumor vasculature and a decrease in tumor vascularity (Levenback et al. 2012).

To date, the *in vivo* observations have been performed in implanted subcutaneous tumors of laboratory animals (mice and rats) so that there remains a need for future studies in a larger mammal, perhaps using sonodynamic therapy for treating naturally occurring cancers. If successful, these additional studies could lead to initial human clinical trials.

ULTRASOUND-MEDIATED CHEMOTHERAPY

In cancer therapy, there is interest in using low-intensity ultrasound to enhance the delivery of chemotherapeutic agents to a solid tumor (Fig. 2, Table 3). The agents may be non-specific in that they do not selectively target neoplastic cells, and thus, high levels of the cytotoxic drug will also be present in normal tissues with possible adverse side effects (Nomikou et al. 2010). Further, factors including poor vascularity and defective lymphatic drainage can result in high interstitial fluid pressure within the tumor and prevent the uptake of therapeutic levels of the drug into the tumor (Nomikou et al. 2010). Insonation of a tumor in the presence of the chemotherapeutic agent provides the potential for

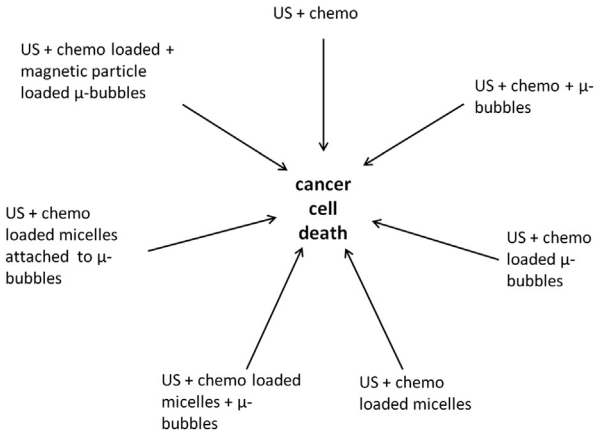

Fig. 2. Outline of different approaches to ultrasound-mediated chemotherapy. Through use of a variety of techniques, low-intensity ultrasound enhances the delivery of chemotherapeutic agents to cancer cells. chemo = chemotherapeutic agent; US = ultrasound; μ-bubbles = microbubbles.

enhancing delivery of the agent to the cancer cells while minimizing the cytotoxic effects in contiguous normal tissues. The delivery of chemotherapeutic agents has been studied in combination with ultrasound alone, with ultrasound and microbubbles and with drug-loaded microbubbles. Additional chemotherapeutic investigations have been made following insonation of drug-loaded liposomes in the presence of microbubbles and ultrasound and insonation of drug-loaded liposomes attached to microbubbles (Table 3). In addition to the role of microbubbles in the delivery of chemotherapy via these direct effects, other effects related to anti-vascular activity have also been described and are discussed later (see Anti-vascular Ultrasound). Also, magnetic microbubbles have been developed in which the drug and iron oxide are co-encapsulated into a microbubble that can be imaged by both ultrasound and magnetic resonance (MR) imaging. This review has centered on the results of recently published research studies; for a general overview of the topic, the reader is referred to articles by Nomikou and McHale (2010) and Trendowski (2014).

Chemotherapy in the presence of ultrasound

The potential for low-intensity ultrasound to increase the sensitivity of cancer cells to a chemotherapeutic agent has been investigated both *in vitro* and *in vivo*.

In vitro *studies.* Insonation of tumor cell suspensions and cultures in the presence of a chemotherapeutic agent can facilitate the cellular uptake of the agent; the inertial cavitation induced by the ultrasound beam leads to the formation of microjets that carry the agent directly into the cell or disrupt the cell membranes, permitting the inflow of extracellularly located agents (Feril and Tachibana 2012).

Yoshida et al. (2008) reported, in human myelomonocytic cells, a synergistic enhancement of cell killing and increased apoptosis when the cells were insonated in the presence of doxorubicin. Only a few studies have evaluated the differences in response between chemosensitive and chemoresistant cancer cells. Yu et al. (2004a) insonated Adriamycin- and cisplatin-resistant substrains of human ovarian cancer cell lines. They observed differing bio-effects between chemosensitive and chemoresistive cells. Cell proliferation and clone formation in the chemoresistive cell populations were suppressed by ultrasound, whereas the chemosensitive cells were unaffected. In another study of doxorubicin, Hassan et al. (2012) studied human uterine carcinoma cells and a multidrug-resistant phenotype. The order of application of insonation and doxorubicin resulted in differences in the sensitivity of the carcinoma cells. The authors observed that either the parent carcinoma cells could be desensitized or the resistant cell could be sensitized to doxorubicin depending on the time of sonication. Insonation of human tongue carcinoma cells in the presence of scutellarin significantly enhanced cell injury, with irregularly shaped and fractured microvilli and formation of apoptotic bodies on scanning electron microscopy; inhibition of cancer cell growth and induction of cell apoptosis occurred (Li et al. 2013).

In vivo *studies.* The efficacy of chemotherapy and ultrasound has also been studied in mouse tumor models. In a murine lymphoma, Tomizawa et al. (2001) found that the combination of intraperitoneal bleomycin and ultrasound leads to suppression of tumor growth. When camptothecin was injected directly into a fibrosarcoma that was then insonated, it was hypothesized that the resultant decrease in tumor growth may have followed the ultrasound-mediated dispersion of the chemotherapeutic drug throughout the tumor, including the more poorly vascularized regions (Nomikou et al. 2010). Chemosensitive and chemoresistant ovarian cancers, implanted in the murine kidney, were insonated 15 min after the intraperitoneal injection of adriamycin (Yu et al. 2004b). Ultrasound potentiated the efficacy of adriamycin in both types of cancer, and thus, it was suggested that ultrasound reversed the adriamycin resistance in ovarian cancer cells. In studies of a human tongue squamous cell carcinoma, scutellarin was orally administered before tumor insonation, and the combined therapy resulted in inhibition of tumor growth, angiogenesis and lymphangiogenesis (Li et al. 2013).

Chemotherapy in the presence of microbubbles and ultrasound

Chemotherapy in the presence of microbubbles and ultrasound has the potential to enhance the *in vivo*

Table 3. Ultrasound-mediated chemotherapy

	Insonation parameter				
In vitro/in vivo	MHz	W cm^{-2}	PW/CW	MPa	Reference
Chemotherapy + US					
In vitro	0.24	5.76	CW		Yu et al. 2004a
	1.0	0.2–0.5	PW	—	Yoshida et al. 2008
	1.0	0.2–0.5	PW	—	Hassan et al. 2012
	1.0	0.05	PW	—	Li et al. 2013
In vivo	1.0	2.0	CW	—	Tomizawa et al. 2001
	0.24	7.84	CW	—	Yu et al 2004 b
	1.0	1.0	PW	—	Nomikou et al. 2010
	1.0	0.01–0.12	PW	—	Li et al. 2013
Chemotherapy in the presence of microbubbles + US					
In vitro	1.0	0.5–1.0	PW	—	Watanabe et al. 2008
	1.0	—	—	0.4–0.8	Escoffre et al. 2011
	1.0	—	PW	0.5	Heath et al. 2012
	0.5–2.25	—	PW	—	Sorace et al. 2012
	1.1	2.0–4.0	CW		Yang et al. 2014
In vivo	1.0	3.0	PW	—	Watanabe et al. 2008
	1.0	3.0	cont	—	Lu et al. 2011
	1.011	0.64	PW		Matsuo et al. 2011
	1.0	—	PW	0.5	Heath et al. 2012
	1.0	—	PW	0.1–2.0	Sorace et al. 2012
Chemotherapy-loaded microbubbles + US					
In vitro	3.0	3.0	PW	—	Chumakova et al. 2006
	1.0	1.0	PW	—	Tinkov et al. 2010b
	1.0	1.0	PW	—	Yan et al. 2011
	5.0	—	PW	0.45	Cochran et al. 2011
	0.8	2.56	PW	—	Ren et al 2013
In vivo	1.3	—	PW	1.2	Tinkov et al. 2010a
	0.3	2.0	PW	—	Kang et al. 2010
	5.0	—	PW	—	Cochran et al. 2011
	1.0	2.0	PW	—	Li et al. 2012c
	1.0	—	PW	0.7	Ting et al. 2012
Chemotherapy-loaded micelles/liposomes + US					
In vivo	1.0	3.4	PW	—	Gao et al. 2005
	1.0	3.4	CW	—	Rapoport et al. 2009
	0.029	5.9	CW	—	Schroeder et al. 2009a
	0.02	1.0	CW	0.173	Staples et al. 2010
	2.25	—	PW	1.9	Yan et al. 2013
Chemotherapy-loaded liposomes in presence of microbubbles + US					
In vivo	1.0	—	—	1.2	Lin et al. 2012a
	1.0	0.3	PW		Zhao et al. 2012
Chemotherapy-loaded liposomes attached to microbubbles + US					
In vitro	1.0	2.0	PW	—	Lentacker et al. 2010
	1.0	2.0	PW	—	Geers et al. 2011
	1.0	—	—	0.2–0.6	Escoffre et al. 2013
In vivo	3.0	2.0	PW	—	Rapoport et al. 2007
Chemotherapy and magnetic nanoparticles co-encapsulated onto microbubbles + US					
In vivo	0.3	2.0	PW	—	Niu et al. 2013

CW = continuous wave; PW = pulsed wave; US = ultrasound; — = parameter not available.

delivery of the agent to a tumor and also to minimize harmful systemic side effects in normal tissues (Heath et al. 2012). Watanabe et al. (2008) observed that the chemo-effect of cisplatin was enhanced in the presence of ultrasound. They believed that at low intensities, the enhanced anti-tumor effect of the chemotherapeutic agent was associated with cavitating microbubbles. At very low intensities, however, it remains to be learned whether the microbubbles collapse or simply undergo volume oscillations. The pressures thus generated caused transient increases in the permeability of cell membranes, allowing exogenous molecules such as chemotherapeutic agents to enter the cell. Further, the intracellular delivery of therapeutic compounds may be facilitated by endocytosis and pore formation involving the endothelial cells lining blood vessels. Meijering et al. (2009) reported that, after insonation (1.0 MHz, 0.22 MPa) of normal rat femoral arteries in the presence of circulating microbubbles, dextran molecules became localized in intracellular vesicles, indicating uptake of macromolecules by endocytosis. Also, endothelial cell pore formation was demonstrated by influx of calcium ions and cellular

release of dextrans. In an *in vitro* study using ultrasound alone (1.5 MHz, 0.3 W cm^{-2}, 0.07 MPa), it was also found that endocytotic vesicles and clathrin (a protein that plays a major role in the formation of coated vesicles) coated pits formed in fibroblasts (Hauser et al. 2009) and again provided a means for the uptake of drugs in addition to sonoporation.

It should also be noted that the release of the chemotherapeutic agent from intravascular microbubbles will also affect the blood vessels, killing the vessels and permitting the therapeutic agent to leave the vessel. The direct effects of microbubbles alone on the vasculature and their role in cancer therapy have been proposed as an anti-vascular therapy (Wood et al. 2007; Goertz et al. 2008, see Section IV). Thus, the relative contributions of chemotherapeutics to the total observed change needs to be determined.

In vitro *studies.* Ultrasound has been applied directly to cell cultures in the presence of microbubbles and a chemotherapeutic agent. When murine colon carcinoma and murine mammary carcinoma cells were insonated in the presence of cisplatin and microbubbles, apoptosis was induced (Watanabe et al. 2008). Also, when head and neck cancer cell lines were insonated in the presence of microbubbles and cisplatin or cetuximab, Heath et al. (2012) reported increased cancer cell permeability and enhanced drug uptake and apoptosis. Sorace et al. (2012) insonated a human breast cancer cell line in the presence of microbubbles, a fluorescent dye (calcein) and taxol, and found that maximum uptake of the extracellular tracer occurred at 1.0 MHz and that cell death was increased by 50% (compared with the controls). They hypothesized that the microbubble-mediated ultrasound therapy increased cell membrane permeability through the generation of small pores, which increased passive intracellular delivery of taxol. Similarly, increased membrane permeability was observed by Yang et al. (2014) after insonation of a human myelogenous leukemia cell line in the presence of doxorubicin and microbubbles. The enhanced delivery of the chemotherapeutic agent resulted in cytotoxicity, cellular necrosis and DNA damage. Their findings supported those of an earlier study by Escoffre et al. (2011), who had reported an increased incidence of apoptosis in human glioblastoma and breast cancer cells after insonation in the presence of doxorubicin and microbubbles.

In vivo *studies.* A reduction in tumor size has been reported with insonation after the chemotherapeutic agent and microbubbles were either injected directly into the tumor or administered intravenously. Cisplatin (*cis*-diamminedichloroplatinum II) and microbubbles were directly injected into human colon carcinoma cells implanted subcutaneously in mice (Watanabe et al. 2008). The tumor was then insonated, and a consequent reduction in tumor volume was observed. Similar studies of a subcutaneous murine melanoma were performed by Matsuo et al. (2011) using melphalon as the chemotherapeutic agent, and again, tumor regression was the result. Lu et al. (2011) also made intratumoral (murine colon cancer) injections of microbubbles before the intravenous injection of epirubicin and tumor insonation. The authors described retarded tumor growth and increased survival times and reported that cavitation contributed to the tumor growth inhibition. Intratumoral injections of microbubbles may not, however, be suitable for clinical practice as access to tumors may not be easy and a uniform distribution of the microbubbles throughout the tumor parenchyma is often difficult to achieve. Observations of the insonation of a squamous cell carcinoma in mice (Heath et al. 2012) after the intravenous injection of cisplatin or cetuximab and a microbubble contrast agent (Definity) revealed a reduction in tumor size, apoptosis and increased cell membrane destruction. Human breast cancer cells were implanted subcutaneously in the flanks of mice, and the resultant tumors were insonated in the presence of intravenously injected microbubbles and taxol (Sorace et al. 2012). A pressure amplitude of 0.5 MPa resulted in the highest impediment to tumor growth over the 3-wk period and also produced the highest degree of tumor necrosis.

Role of microbubbles in opening blood–brain barrier for cerebral chemotherapy. There is increasing interest in the use of focused ultrasound in the presence of circulating microbubbles to temporarily open the blood–brain barrier (BBB). The barrier is characterized by tight junctions between the endothelial cells lining the blood vessels in the central nervous system so that the passage of nutrients into the brain via cellular pathways can be closely regulated and brain homeostasis can be maintained. Further, the barrier also prevents toxic substances as well as other pathogens from entering the brain. Temporarily increasing the permeability of the barrier will permit the passage of chemotherapeutic agents into the neural tissue, and it is this feature that is of particular relevance in cancer therapy. The underlying bio-effect of insonation is stable cavitation as energy is transferred to the circulating microbubbles, causing them to expand and contract (oscillate) with resultant damage to the contiguous endothelial cells and their tight junctions with resultant increases in the permeability of the BBB. The topic has recently been extensively reviewed by Burgess and Hynynen (2014) and Liu et al. (2014). In Table 4, other recent publications are listed together with the insonation parameters that were used to increase the permeability of the barrier in normal rodent brains and in those with implanted cerebral neoplasms.

Table 4. Opening of blood–brain barrier with pulsed focused ultrasound and microbubbles in rodents

	Insonation parameter			
	MHz	W cm^{-2}	MPa	Reference
Normal brain	0.4	5.0–10.0	0.98–1.35	Liao et al. 2012b
	—	—	0.45–0.60	Chen et al. 2013b
	1.5	—	0.45–0.60	Samiotaki and Konofagou 2013
Implanted brain tumor				
Glioma	0.4	1.0–10.0	0.45–1.35	Liu et al. 2010
Breast cancer	0.69	0.32	0.69	Park et al. 2012
Glioma	1.0	—	0.7	Ting et al. 2012
Gliosarcoma	1.7	—	1.2	Treat et al. 2012
Glioma	0.69	—	0.55–0.81	Aryal et al. 2013
Glioma	0.40	4.0	0.325	Fan et al. 2013a
Glioma	1.0	3.0	0.6	Wei et al. 2013
Glioma	0.61	—	0.4	Kovacs et al. 2014
Astrocytoma (unfocused US)	0.5	—	0.4	Kovacs et al 2014

US = ultrasound.

In normal rat brains, Liao et al. (2012b) used MR imaging to reveal regions of breakdown of the BBB after cerebral insonation in the presence of albumin-shelled Gd-DTPA circulating microbubbles and found that a threshold acoustic pressure of 0.98 MPa was required to open the BBB. In further MR observations, Samiotaki and Konofagou (2013) reported an opening threshold in mice of 0.45 MPa in the presence of circulating Definity microbubbles. A similar threshold was also found in mice (Chen et al. 2013b) in which at 0.45 MPa there was a homogeneous breakdown of the BBB in the insonated hippocampus in the presence of circulating microbubbles. Additional observations with circulating phase-shift nanodroplets (formed by pressurizing microbubbles so that the gas core was converted into a liquid phase) revealed that higher acoustic pressures were required to open the BBB, but the incidence of inertial cavitation was reduced (Chen et al. 2013b).

Further *in vivo* observations have been made in rodents after chemotherapy of implanted brain neoplasms. Liu et al. (2010) used MR imaging to follow tumor progression after opening of the BBB by focused sonication in the presence of circulating microbubbles and treatment with carmustine (bis-chloroethylnitrosourea). Tumor growth was controlled, and animal survival times were increased. In another study, carmustine was loaded onto microbubbles, and brain insonation released the chemotherapeutic agent at the target site (Ting et al. 2012). MR imaging revealed control of tumor progression, and improved animal survival times were again observed. In multiple investigations using doxorubicin (either alone [Kovacs et al. 2014], encapsulated in liposomes [Aryal et al. 2013; Treat et al. 2012] or conjugated with supermagnetic iron oxide nanoparticles [Fan et al. 2013a]), focused ultrasound therapy of a brain neoplasm in the presence of microbubbles also resulted in reduced tumor growth and an increase in median animal survival times. These observations have also been confirmed using other chemotherapeutic agents including trastuzumab (Park et al. 2012; treatments given weekly for 6 wk) and temozolomide (Wei et al. 2013). Burgess and Hynynen (2014) have, however, raised the concern that the intravenous drug concentrations selected for a successful therapeutic outcome in the brain may have to be adjusted to avoid potential peripheral toxicity.

It should, however, be noted that the normal BBB is damaged by a brain neoplasm, and this is the reason that iodine-containing contrast agents, in the case of computed tomography, and paramagnetic contrast agents, in the case of magnetic resonance imaging, can cross the leaky barrier and reveal the cerebral pathology in each of these imaging systems. Thus, the future clinical role of ultrasound therapy may be to further increase the permeability of an already leaky barrier and perhaps permit the egress of larger chemotherapeutic molecules than is normally possible from the vascular lumen into the cancer tissue.

Chemotherapy-loaded microbubbles and ultrasound

The chemotherapeutic drug may be loaded or bound to a microbubble whose diameter is less than that of an erythrocyte so that it easily enters the neovasculature of a tumor (Liu et al. 2006b). On insonation of a tumor, ultrasound targeted microbubble destruction occurs, which has the advantages of being externally controlled and localized to the tumor site. The formation of microbubbles and their potential as carriers for drugs, small molecules, nucleic acids and proteins have been reviewed by Tinkov et al. (2009). The structure of the shell of microbubbles is important; lipophilic chemotherapeutic drugs including doxorubicin, paclitaxel and docetaxel can be incorporated into the lipid layer of a microbubble (Kang and Yeh 2012). It is believed that such soft-shelled microbubbles may be not be capable of stably incorporating large volumes of drug molecules because of their relatively thin shells; the use of polymer-based hard-shelled microbubbles permits the entrapment of hydrophilic (rhodamine-B) and hydrophobic (coumarine-6) chemotherapeutic agents in the shell and may enhance the efficacy of cancer therapy (Fokong et al. 2012).

The concept of a theranostic microbubble which can combine a chemotherapeutic role with ultrasound imaging is receiving increased attention (Peyman et al. 2013; Zhao et al. 2013). The bubble is loaded with a chemotherapeutic agent that is released into a tumor under the action of low-intensity ultrasound; the bubbles may also act as a contrast agent and be used for contrast-

enhanced power Doppler ultrasound imaging of the tumor vasculature. Stride and Coussios (2010) have provided an extensive review of the basic physics and cavitation of microbubbles used in therapy and imaging and how, when acoustically driven, they can be destroyed at a tumor site and release a chemotherapeutic agent. The mechanism underlying the delivery of a drug from the microbubble to a tumor was investigated using a light-emitting compound loaded onto a microbubble (Liao et al. 2012a). On insonation (1 MHz, pulsed, 3.0 W cm^{-2}), the compound was released into tumor capillaries and entered the neoplastic cells.

The incorporation of drugs onto the surface of microbubble has been described (Ferrara et al. 2009; Liu et al. 2006b; Mayer et al. 2008). During tumor insonation, cavitation ruptures the bubble, thus releasing the drug and delivering it into the tumor—it may impart a "ballistic effect" to drive the drug through the wall of the tumor capillary (Liu et al. 2006b). Also, sonication can oscillate the microbubbles, resulting in an increase in the permeability of the contiguous cell membranes, including those of the endothelial cells lining tumor capillaries, and can further enhance the entry of a locally released chemotherapeutic agent into a cancer cell (Feril and Tachibana 2012; Stride and Coussios 2010; Zhao et al. 2013). After insonation (1.5 MHz, pulsed, 1.0 W cm^{-2}) of a rat glioma cell culture, fibered confocal fluorescence microscopy revealed in real time the intracellular delivery of an impermeable green dye from the microbubble into the cancer cell (Derieppe et al. 2013).

In vitro *studies.* Insonation, in the presence of microbubbles, of a breast cancer cell line treated with 5-fluorouracil resulted in damage to the cells, and it was presumed that the chemotherapeutic agent bound to the albumin shell of the microbubble (Chumakova et al. 2006). Doxorubicin was embedded in the shell of the microbubble, and its insonation in a culture of human renal carcinoma cells resulted in enhanced cytotoxic activity compared with that of free doxorubicin and doxorubicin-loaded liposomes (Tinkov et al. 2010b). Yan et al. (2011) studied the bio-effects of paclitaxel-loaded lipid microbubbles coated with a breast tumor-homing peptide; the microbubbles attached to human breast cancer cells, and insonation of the culture resulted in reduced cell viability. Using a polymer microbubble, Cochran et al. (2011) found that paclitaxel could be loaded to a much greater extent than doxorubicin, and on insonation of cultures containing loaded microbubbles and human breast cancer cells, there was significant release of paclitaxel, presumably as the microbubbles ruptured, leading to the observed reduction in cell viability. Ren et al. (2013) encapsulated docetaxel, a hydrophilic molecule, in a lipid microbubble and found that insonation inhibited the proliferation of human colon carcinoma cells.

In vivo *studies.* In power Doppler ultrasound images of liver cancer in rabbits, Cochran et al. (2011) found that doxorubicin-loaded microbubbles could permeate the vasculature of the tumor. Their observation confirmed the findings of Tinkov et al. (2010a), who used doxorubicin-loaded microbubbles to treat a murine pancreatic carcinoma that had been implanted subcutaneously in rats. After insonation, there was a reduction in the tumor growth rate related to an increase in local drug concentration. In comparison to the untreated controls, a reduction in tumor growth rate, accompanied by an increased survival time and reduction in the number of metastases, was also reported in a liver tumor in rabbits insonated after the intravenous injection of docetaxel-loaded lipid microbubbles (Kang et al. 2010); ultrasound therapy ruptured the microbubbles and released the drug locally in the tumor tissues.

When 10-hydroxycamptothecin-loaded microbubbles were injected intravenously, they were also detectable in power Doppler images of a subcutaneously located murine hepatic tumor (Li et al. 2012a). During insonation of the tumor, the microbubbles fragmented into nanoparticles, the fragments accumulated in the tumor and the chemotherapeutic agent was slowly released. The low blood flow in tumors and their large blood volume favored the infusion and destruction of microbubbles within the tumor. Significant drug levels were delivered locally, and the growth rate of the tumor was reduced; there was, however, no reduction in the size of tumors receiving unloaded microbubbles.

Chemotherapy-loaded polymeric micelles or liposomes and ultrasound

An alternative approach to loading a chemotherapeutic agent onto a microbubble is to instead use a polymeric micelle or liposome. These micelles have been used to improve the delivery of chemotherapeutic drugs to a tumor; the aim is to release the agent from the micelle under the action of ultrasound. The topic of ultrasound activation of micelles has recently been reviewed (Husseini and Pitt 2009; Rapoport 2012; Schroeder et al. 2009b). It has been postulated that inertial cavitation improves micelle delivery by creating holes in the membranes of neoplastic cells so that the micelles can diffuse into the neoplastic cells. Inertial cavitation may also open the micelles to release the now intracellular chemotherapeutic drug (Husseini and Pitt 2009). It has also been suggested that the insonation induces a mild hyperthermia that may enhance the movement of the micelles from the tumor capillaries into the interstitium of the tumor (Rapoport 2012).

There have been a series of *in vivo* observations of the effectiveness of the therapy method. Schroeder et al. (2009a) reported that insonation of a colon adenocarcinoma implanted in the feet of mice after intravenous injection of cisplatin-loaded liposomes inhibited tumor growth, and the tumors regressed over time. In studies of intraperitoneal or subcutaneous ovarian carcinomas in mice, Gao et al. (2005) reported that ultrasound triggered intracellular uptake of polymeric micelles encapsulated with doxorubicin; the drug had previously been injected intravenously and had accumulated in the interstitium of the tumor. The growth rate of the subcutaneous tumor also decreased. Further, Yan et al. (2013) intravenously injected liposome–microbubble complexes containing paclitaxel before insonation of mice with a subcutaneous breast tumor. They reported an increase in drug concentration in the tumor and inhibition of tumor growth.

In a subcutaneous colorectal epithelial cancer cell line in rats, Staples et al. (2010) reported that the infusion of doxorubicin-labeled micelles and insonation (20 kHz, continuous, 1.0 W cm^{-2}, and 476 kHz, pulsed, 23.61 W cm^{-2}) led to higher concentrations of the chemotherapeutic agent within the tumor for 30 min post-insonation; at later times, similar levels of the agent were present in insonated and non-insonated tissues. The authors suggested that cavitation events may have released the doxorubicin from circulating and extravasated micelles into the tumor, and insonation could have transiently increased the permeability of the tumor neovasculature. With the progression of time, however, cavitation could occur at slower rates as the micelles are cleared from the circulatory system; also, the tumor capillaries will regain their normal permeability, thus explaining the similar levels of doxorubicin observed in cancerous and normal tissues.

Rapoport et al. (2009) followed a different approach in which nano-micelles loaded with paclitaxel or gemcitabine were infused into the tumor vasculature and transformed by ultrasound into microbubbles after the nano-emulsions had extravasated into the interstitium. Ovarian, breast and pancreatic cancers were studied in mice, and the results indicated enhanced delivery of the chemotherapeutic agents to the tumors. There was also a reduction in tumor growth; although the initial reduction was significant, subsequent treatments were less effective, possibly because of the development of drug resistance by the cancer cells.

To minimize the potential side effects a chemotherapeutic agent on normal tissues, Ibsen et al. (2012) developed "shockwave ruptured nanopayload carriers" in which a microbubble was encapsulated with a protective outer liposome. Tissue phantom studies were performed using 2.25 MHz ultrasound at the relatively higher pressure amplitude of 1.5 MPa. Insonation destroyed the microbubble of perfluorocarbon gas and ruptured the outer liposome membrane, and so had the potential to release a highly concentrated chemotherapeutic payload from within the particle.

Chemotherapy-loaded liposomes in the presence of microbubbles and ultrasound

Inertial cavitation induced by the insonation of microbubbles can augment the intracellular absorption of a chemotherapeutic agent. Zhao et al. (2012) insonated breast cancer cells in the presence of microbubbles and doxorubicin-loaded liposomes; they reported that ultrasound mediated cavitation lead to the observed reduction in cell viability in the treated cell cultures. In an *in vivo* study, Lin et al. (2012a) used polyethylene glycol-coated liposomes loaded with doxorubicin to treat a murine colorectal adenocarcinoma implanted subcutaneously in mice. Microbubbles were injected intravenously, and the tumor was insonated at a pressure amplitude of 1.2 MPa, before injection of the chemotherapeutic agent. After therapy, there were significantly enhanced drug levels in the tumor and delayed tumor growth. Also, it was found in other experiments that the temperature of the tumor increased by 5.0°C when insonation occurred in the presence of circulating microbubbles, but by only 2.5°C in their absence. It was concluded that the absorption of ultrasound energy was enhanced by the oscillation and cavitation of microbubbles within the insonated tumor. Zhao et al. (2012) used an intratumoral injection of microbubbles and an intravenous injection of doxorubicin-loaded liposomes and found that the growth of breast cancer tumors in mice was reduced when insonated. It was also concluded that cavitation was an important bio-effect of insonation and enhanced the absorption of doxorubicin.

Chemotherapy-loaded liposomes attached to microbubbles and ultrasound

The feasibility of the targeted delivery of a theranostic agent under image guidance is addressed by the attachment of drug-loaded liposomes to a microbubble of ultrasound contrast medium. Diagnostic ultrasound can be used to confirm the presence of the loaded microbubbles within the tumor vasculature; the application of low-intensity ultrasound then ruptures the bubbles, accurately restricting the delivery of the chemotherapeutic agent to the neoplastic cells.

The cytotoxicity of doxorubicin-containing liposomes coupled to the surface of microbubbles has been illustrated *in vitro*. Lentacker et al. (2010), using melanoma cells, described an almost instantaneous cellular entry of the chemotherapeutic agent after insonation, which was thought to be related to sonoporation of cell

membranes. In a subsequent study also of melanoma cells, Geers et al. (2011) reported that 600–1300 doxorubicin-loaded liposomes were attached to the surface of each microbubble, and insonation increased the killing of the cancer cells. In another study of glioblastoma cells, insonated in the presence of similar liposomes linked to microbubbles, Escoffre et al. (2013) reported a decrease in cancer cell viability.

The therapeutic potential of combining drug-loaded liposomes, microbubbles and ultrasound was observed by Rapoport et al. (2007) when polyethylene glycol-coated liposomes loaded with doxorubicin and perfluoropentane microbubbles were used to treat breast cancer tumors in mice. After intravenous injection of the liposome/microbubble mixture and subsequent insonation, increased uptake of doxorubicin into the tumor was observed. The uptake of the drug was greater when microbubbles and drug-loaded liposomes were used than when the liposomes were administered alone. The observed increase was attributed to inertial cavitation. Heating of tissue to 41°C was also observed in normal mice by Cool et al. (2013) when indocyanine green-containing liposomes were coupled to the surface of intravenously injected microbubbles; insonation (1 MHz, 2.0–5.0 W cm^{-2}) caused release of the dye, and it was concluded that the technique may have applications in improving ultrasound-mediated drug delivery.

An alternative approach has been reviewed by Ibsen et al. (2013) in which the chemotherapeutic agent is carried on the surface of the microbubble, and the loaded microbubble is in turn encapsulated within a liposome. Potential advantages include the rapid release of the encapsulated chemotherapeutic drug within the tumor and a low leak rate of the agent into normal tissues. The microbubble can also be used as an imaging contrast agent, that is, theranostic agent, as it is involved in both therapy and diagnosis.

Chemotherapy in the presence of ultrasound and magnetic nanoparticles loaded onto microbubbles (magnetic microbubbles)

The encapsulation of iron oxide nanoparticles into microbubbles enabled the development of multimodality imaging, that is, (MR imaging in addition to ultrasound imaging; the topic has recently been briefly reviewed (Owen et al. 2012; Zhao et al. 2013). Niu et al. (2013) developed such a multifunctional theranostic agent in which pelvic limb lymph node metastases from an implanted squamous cell carcinoma in rabbits were imaged by both MR and ultrasound. Doxorubicin and iron oxide nanoparticles were co-encapsulated into microbubbles, and insonation of the nodes triggered release of the chemotherapeutic agent. The therapy increased apoptosis and decreased tumor proliferation and micro-blood vessel and lymphatic density.

Additional comments

In summary, investigations of ultrasound-mediated chemotherapy have evaluated the efficiency of the delivery of a wide range of chemotherapeutic agents to cancer cell cultures and suspensions and solid tumors. Across all delivery methods, consistent findings have been a potentiation of the efficacy of the delivery of chemotherapeutic agents with resultant necrosis of neoplastic cells, inhibition of tumor growth and increased animal survival times. The precise mechanisms underlying ultrasound-mediated chemotherapy are, however, frequently based on speculation rather than direct evidence. The insonation of a solid tumor with low-intensity ultrasound in the presence of an intravascular chemotherapeutic agent can potentiate and localize the cytotoxic affects to the cancer cells, while minimizing side effects in the adjacent normal tissue. Traditional chemotherapy is given in low doses over time, and future studies may determine whether ultrasound-mediated chemotherapy can substantially reduce the overall dose of the agent and decrease its toxicity. Although some *in vivo* experimental studies have used intratumoral or intraperitoneal injections of the chemotherapeutic agent or microbubbles, intravenous injections should result in a more even and generalized distribution of these substances within the tumor and an improved response to therapy.

Although large numbers of studies have reported the efficacy of ultrasound-mediated chemotherapy, relatively few have dealt with the issue of the biodistribution of the agents and their elimination from the body. Those chemotherapeutic agent-loaded microbubbles not destroyed by an ultrasound beam that has been localized to a tumor will continue to circulate in the vascular system and may be retained in a major organ. Toft et al. (2006) studied the biodistribution of the perfluorobutane gas contained in a microbubble at different time points after its intravenous injection into rats. They observed that the highest concentration of perfluorobutane was in the spleen, followed by decreasing levels respectively in the liver, lung, kidney and other tissues. They also reported that 50% of the perfluorobutane was recorded in the exhaled air by 20 min after injection, and 96% was recovered in 24 h. Retention of microbubbles in the sinusoidal spaces within the liver has been reported, and they are phagocytosed by Kupffer cells (liver-specific macrophages) (Cosgrove 2006; Liu et al. 2008a; Yanagisawa et al. 2007). In *in vitro* studies, acoustic pressures of 0.63 MPa were required to destroy microbubbles adherent to Kupffer cells, and 0.73 MPa destroyed those microbubbles that had been phagocytosed (Liu et al. 2008a). Microbubbles are also taken up by the spleen, where they may be phagocytosed

by macrophages or simply trapped within the splenic parenchyma (Lim et al. 2004). Further, it has been reported that lipid-shelled microbubbles are retained in the renal cortex of mice and humans (Liu et al. 2013b). The microbubbles were located in the murine glomerular microvessels after a complement-mediated interaction with the vascular endothelium.

Given that the majority of the microbubbles are destroyed during insonation of the tumor neovasculature, it is likely that non-clinically significant levels of the chemotherapeutic agent will be retained in the liver, spleen or kidney. In considering future developments in ultrasound-mediated chemotherapy, it will be important, however, to fully understand the behavior and eventual outcome of these phagocytosed or adherent microbubbles, especially as their associated chemotherapeutic agent has the potential to cause toxic side effects in these major organs.

Whether by diagnostic ultrasound or by MR imaging, the ability to image the distribution of the chemotherapeutic agent within the tumor has significant clinical implications. By loading the chemotherapeutic agent onto the surface of a microbubble of ultrasound contrast medium, localized insonation of such a theranostic agent could lead to accurate delivery of the drug to a tumor and minimization of unwanted cytotoxic effects in the adjacent normal tissues. Further, it may be feasible to reduce the systemic dose of the chemotherapeutic agent, leading to a reduction in clinical side effects. In considering the underlying bio-effects of such theranostic methods, the emphasis has been placed on the role of inertial cavitation; little attention has been given, however, to other possible mechanisms including accompanying thermal effects on the tumor vasculature. As the *in vivo* studies have usually been performed in rat and mouse tumor models, there is a need to progress to investigations in naturally occurring neoplasms which could then lead to initial clinical trials.

ULTRASOUND-MEDIATED GENE TRANSFECTION

Recently there has been considerable interest in the emerging area of using ultrasound and microbubbles to facilitate gene delivery to neoplastic cells (Feril et al. 2006; Geis et al. 2012; Liang et al. 2010; Sirsi and Borden 2012). It has been hypothesized that the use of focused ultrasound to target DNA-loaded microbubbles located within the lumen of a tumor's neovasculature can result in destruction of the microbubbles and release or transfection of genetic material locally into the tumor parenchyma. It is further proposed that insonation also causes the process of sonoporation in which transient pores form in the cancer cell membranes through which molecules are able to enter the cell (Haag et al. 2006; Li et al. 2014). In each case, insonation is considered to be the driving force responsible for transfection of the nucleic acids and the subsequently observed therapeutic effects in the cancer cells. It remains uncertain, however, as to exactly how genes pass through the endothelial barrier to reach the tumor. Sporadic capillary rupture and increased vascular permeability, as well as enhanced permeability of cell membranes, may play a role in the observed efficacy of therapy. Some of the more recent studies are listed in Table 5; the acoustic pressures required to promote gene transfection are usually greater than 0.3 MPa and so fall into a general classification of moderate ultrasound intensities. We have provided an introductory, preliminary review of the topic, and the reader is encouraged to evaluate the results of new investigations as further data accumulate.

As a routine, gene therapy was easily targeted to a tumor, and the investigations revealed successful transfection of genetic material resulting in apoptosis of cancer cells, both *in vitro* and *in vivo*, and reduced tumor growth. After insonation, the wide distribution of transfection within the tumor led to a more efficient therapeutic response; Fujii et al. (2013) were unable to detect transfection in organs outside ultrasound beams. Microbubbles loaded with genes or inhibiting RNA (directed to epidermal growth factor) have been found to effectively reduce tumor growth (Carson et al. 2011, 2012). The underlying hypothesis is delivery of genes that inhibit signaling processes to specific sites in the tumor while sparing non-targeted areas. By this approach, selective payloads of these materials can be delivered non-invasively and repeatedly.

On some occasions, the genetic material and microbubbles were injected separately into a tumor (Tang et al. 2012), or alternatively, they were mixed and then added to the tissue culture or injected into the tumor (Li et al. 2012b, 2014; Sakakima et al. 2005; Yamaguchi et al. 2011a; Zhang et al. 2011; Zolochevska et al. 2011). An improved distribution throughout the parenchyma of the tumor would, however, be expected when the nucleotide and microbubble are linked and injected intravenously. As the phosphate backbone of DNA and RNA is highly anionic, microbubbles with cationic shells have been used so that there is spontaneous formation by electrostatic binding of a complex based on the charge interactions (Wang et al. 2012a; Yu et al. 2013). In using such complexes, Wang et al. (2012a) reported significantly enhanced transfection in both cell cultures and tumors. They observed that the enhancement in transfection efficiency with cationic microbubbles was more pronounced in cell culture studies than in tumors. Possibly more DNA was delivered in tissue cultures

Table 5. Insonation parameters used for ultrasound- and microbubble-mediated gene delivery

Cells/tumor	Insonation parameter					Treatment	Reference
	MHz	W cm^{-2}	MI	MPa	PW/CW		
In vitro							
Hepatocellular carcinoma	1.0	0.5	—	—	PW	Interferon β	Sakakima et al. 2005
Prostate	1.75	—	1.9	1.44*	PW	Anti-sense oligodeoxynucleotide	Haag et al. 2006
Hepatoma	1.0	1.0	—	—	PW	pEGFP	Zhang et al. 2011
Prostate	0.021	4.6	—	—	PW	pEGFP DNA	Bai et al. 2012b
Endothelial cell	1.0	2.0	—	—	PW	Click beetle luciferase	Wang et al. 2012a
Breast cancer	2.0	0.75	—	—	CW	KDRP-CD/TK	Li et al. 2012b
Ovarian	1.0	0.5	—	—	PW	PEGFP-N1-wtp53	Chang et al. 2013
In vivo							
Hepatocellular carcinoma	1.0	2.0	—	—	PW	Interferon β	Sakakima et al. 2005
Prostate	—	—	1.9	—	PW	Anti-sense oligodeoxynucleotide	Haag et al. 2006
Hepatoma	1.0	2.0	—	—	PW	HSV-TK	Zhou et al. 2010
Squamous cell carcinoma	1.3	—	1.6	1.40*	PW	TK	Carson et al. 2011
Melanoma	1.011	0.22	—	—	PW	Interferon β	Yamaguchi et al. 2011a
Prostate	1.0	1.0	—	0.12	PW	Interleukin-27	Zolochevska et al. 2011
Squamous cell carcinoma	1.3	—	1.6	1.40*	PW	sIRNA	Carson et al. 2012
Nephroblastoma	1.0	1.0	—	—	CW	DNA	Sirsi et al. 2012
Hepatic	1.0	3.0	—	—	PW	KDR-TK, AFP-TK	Tang et al. 2012
Endothelial cell	1.0	2.0	—	—	PW	Click beetle luciferase	Wang et al. 2012a
Mammary adenocarcinoma	1.3	—	—	2.1	PW	shRNA	Fujii et al. 2013
Hepatoma	1.3	—	1.3	1.14*	PW	HSV-TK/GCV	Yu et al. 2013
Renal carcinoma	1.0	2.0	—	—	PW	Recombinant adeno-associated virus	Li et al. 2014

CW = continuous wave; MI = mechanical index; PW = pulsed wave; — = parameter not available.

* Represents calculated negative peak pressure = MI $*$ $\sqrt{\text{frequency}}$.

than *in vivo*, but a further reason for the difference could be the extent of cavitation activity: there may have been more cavitation *in vitro* than *in vivo*.

In these ultrasound-mediated methods, the transfection/transduction of genetic material was usually accomplished using non-viral techniques, but use of a virus as a carrier with microbubbles was also successful (Li et al. 2014; Tang et al. 2012). Compared with viral vectors, non-viral techniques have increased tolerability, but are disadvantaged by low transfection efficiencies (Wang et al. 2012a); however, microbubbles are good carriers of genes with a greater capacity for anti-sense oligonucleotides and fragments of DNA and even the entire chromosome (Li et al. 2012b).

As far as the underlying bio-effects are concerned, during insonation, the *in vivo* cavitation activity is confined to microbubbles within the lumens of the tumor neovasculature, and it remains to be elucidated how these cavitation events induce sonoporation and vesicle formation in the extravascularly located cancer cells. In summary, ultrasound-mediated gene therapy is non-invasive, and repeated delivery can be used to achieve a more sustained transfection; also, multiple genes can be delivered to achieve a synergistic therapeutic response (Fujii et al. 2013). The method is site specific, thus providing a distinct advantage over systemic cancer therapies for tumors with their associated effects on normal tissues (Carson et al. 2012; Sirsi et al. 2012). It should, however, be remembered that after insonation, the transfection of genes could result in unexpected morphologies and abnormalities in normal cells contiguous with the tumor. In the future, animal investigations could be aimed at following tumors over longer periods post-therapy and making repeated deliveries of genetic material. Also, a multigene approach using a combination of anti-angiogenic and pro-apoptotic gene therapies could be useful (Fujii et al. 2013).

ANTI-VASCULAR ULTRASOUND

It has been proposed that a solid tumor should be considered to have two compartments of cells, one containing the neoplastic cells and the other the endothelial cells of the tumor neovasculature (Folkman 2001; Siemann 2006). As a solid tumor exceeds a cubic millimeter in volume, it must establish its own vascular supply to ensure the continuing viability of its cancer cells. It is well established that the tumor neovasculature differs in structure from that of normal blood vessels: tumor vessels are fragile and leaky and have abnormal branching patterns (Vaupel 2006).

Ultrasound imaging using circulating microbubbles has become the method of choice to visualize the tumor neovasculature and to differentiate between vascular and avascular regions within a tumor (Anderson et al. 2011; Chen et al. 2013c; Hyvelin et al. 2013; Perini et al. 2008; Wood et al. 2005, 2006). The technique can also be used to assess the efficacy of an anti-vascular therapy. After the intravenous injection of microbubbles, the vascular regions within a tumor can be identified in

contrast-enhanced B-mode images (delta-projection imaging [Sehgal et al. 2009]) and power Doppler images (visual inspection, percentage area of flow and color weighted flow area, cumulative histogram area [Mason et al. 2011; Wood et al. 2007]). Alternative approaches using high-frequency Doppler imaging without the use of microbubbles have also been developed. Goertz et al. (2002) and Chen et al. (2011, 2012a) observed the vascularity of murine tumors in power Doppler images made at 25–38 MHz, and in a study of a prostatic adenocarcinoma implanted in mice, Chen et al. (2013b) assessed vascular perfusion at 25 MHz in power Doppler images by measuring the ratio of the color weighted pixels to the total tumor area or percentage area of flow.

This review centers on techniques using the combination of ultrasound and microbubbles as a vascular disrupting agent (Fig. 3); the tumor vasculature is damaged, leading to necrosis of the neoplastic cells with a consequent reduction in tumor growth and lengthened survival time. Although this review is focused on the role of low-intensity ultrasound as part of such an anti-vascular tumor therapy, we have also included references to the use of moderately higher intensity insonations (Table 6). The anti-vascular responses to these differing approaches are probably related to major differences in their bio-effects: lower intensities are reported to create more thermal effects, and higher intensities, more cavitation effects. Such divisions, however, may be considered artificial as the two effects are intertwined, and seldom is it true that one class of effects can be disregarded (Baker et al. 2001).

Predominantly thermal bio-effects

In multiple studies of a murine melanoma model, it was consistently found that tumor insonation (1- to 3-min treatment time) in the presence of circulating microbubbles had a significant anti-vascular effect (Wood et al. 2005, 2006, 2007, 2008, 2010). Each minute of insonation decreased tumor perfusion by ≈25% (Wood et al. 2005). Of particular interest in these theranostic studies was the observation that the normal vasculature in the adjacent tissues and organs appeared unaffected by the therapy. The tumor increased in echogenicity after therapy; it appeared to be related at least in part to tissue inhomogeneities formed after disruption of the tumor neovasculature (Wood et al. 2009). In detailed histologic observations, the predominant effect of insonation was an irreparable dilation of the tumor capillaries with associated intercellular edema (Bunte et al. 2006). There were also hemorrhage and increased intercellular fluid. A day after insonation, liquefactive necrosis of the neoplastic cells had occurred and was related to a generalized tumor ischemia following the effects of therapy on the neoplasm's vascular channels. It should be noted that this histologic finding differs from that reported after tumor insonation with high-intensity focused ultrasound, where acute coagulative necrosis occurs, not only of the neoplastic cells, but also of the tumor vasculature (Van Leenders et al. 2000; Wu et al. 2001, 2002). These observed bio-effects resulted in reduced tumor growth rate and a 28% increase in survival time after a single 3-min tumor therapy session (Wood et al. 2010). The anti-vascular action of low-intensity ultrasound was increased when tumor insonation was at 3 MHz rather than 1 MHz, and the temperature of the tumor increased by 5°C and 2°C min^{-1}, respectively (Wood et al. 2008). Thus, it was considered that a thermal effect on the endothelial cells lining the tumor capillaries may be important, although other bio-effects, sonochemical reactions and cellular responses could also play a role (Wood et al. 2005, 2008). In recent studies, Hunt et al. (2014) found that the effects of anti-vascular ultrasound go beyond direct cytotoxicity to include intratumoral immune activation.

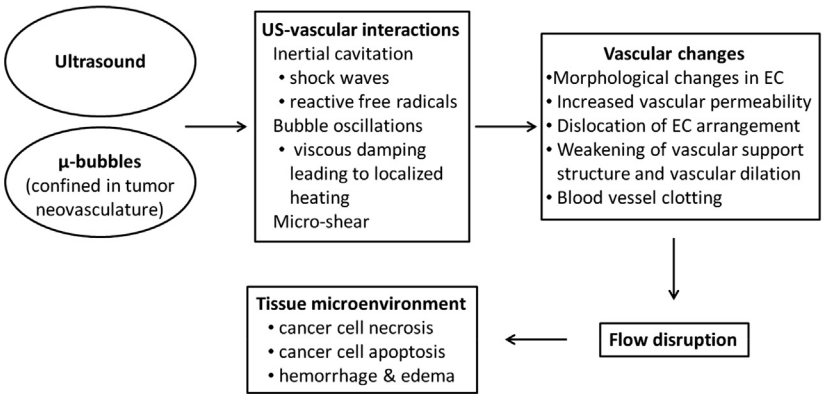

Fig. 3. Schema of anti-vascular ultrasound. Microbubbles contained in the neovasculature of a tumor are insonated with low-intensity ultrasound, causing a series of bio-effects that lead to vascular damage. Blood flow to the tumor is disrupted and, consequently, necrosis and apoptosis of cancer cells occur. EC = endothelial cell; US = ultrasound; μ-bubbles = microbubbles.

Table 6. Anti-vascular ultrasound therapy of tumors in the presence of circulating microbubbles

Type of microbubble	Tumor	Insonation parameter				Reference
		MHz	W cm^{-2}	PW/CW	MPa	
Unloaded	Melanoma	1.0–3.0	2.0	CW	0.28	Wood et al. 2005, 2006, 2007, 2008, 2010
	Three tumor types	1.0	—	PW	0.74	Goertz et al. 2008, 2009
	Adenocarcinoma	1.2	—	PW	5.0	Chin et al. 2009
	Colon carcinoma	1.5	133*	—	—	Zhong et al. 2010
	Glioma	1.0	—	PW	1.0–1.2	Burke et al. 2011
	Adenocarcinoma	1.0	2.0	PW	—	Lin et al. 2012a
	Walker-256	0.83	0.4, 1.36	PW	2.6, 4.8	Liu et al. 2012
	Colon carcinoma	0.24	—	PW	0.5	Huang et al. 2013
	Hepatoma	1.75	539	—	—	Wang et al. 2013a
	Breast cancer	5.0	—	PW	4.0	Hu et al. 2012
	Epidermoid	1.22	0.89	PW	4.6	Peijing et al. 2014
Unloaded + anti-angiogenic genes	Prostate	1.0	2.0	PW	—	Duvshani-Eshet et al. 2007
	Hepatoma	1.0	2.0	PW	—	Nie et al. 2008
Loaded						
Docetaxel	Squamous carcinoma	0.3	2.0	—	—	Kang et al. 2010
Docetaxel	Prostate	1.0	—	PW	1.65	Goertz et al. 2012
Doxorubicin	Breast cancer	3.0	2.0	PW	—	Rapoport et al. 2007
Doxorubicin	Colorectal	1.0	2.0	PW	0.6	Lin et al. 2012b
Carmestine + anti-angiogenic complex	Glioma	1.0	—	PW	0.5	Fan et al. 2013b
Anti-angiogenic agent	Colon cancer	0.24	—	PW	0.5	Zhang et al. 2014

CW = continuous wave; PW = pulsed wave; — = details not provided.
* Estimated.

In modeling blood flow in a tumor, Levenback et al. (2012) considered the tissue as a continuum of microbubble-filled vasculature, cells and interstitial fluids with compressibility equal to the sum of the compressibilities of each component. The mathematical simulations established that the absorption of ultrasound by viscous dampening of the microbubble oscillations induced local heating of the neovasculature. Microbubble-enhanced heating was also modeled and observed in a phantom by Razansky et al. (2006). Blood flow is slower in tumor neovasculature than in the normal vasculature of healthy tissues, and thus, in tumors there is additional time for an interaction between ultrasound and microbubbles with resultant thermally induced damage to endothelial cell linings, leading to the observed anti-vascular effect of therapy (Levenback et al. 2012). Such damage will be significantly diminished in normal capillaries where the circulation is faster and any temperature rise will be much smaller and have no biological effect.

In a study of normal rabbits, McDannold et al. (2006) insonated the brain using 1.5-MHz focused, continuous and pulsed ultrasound in the presence of circulating microbubbles. Small focal regions (1 mm in diameter) were sonicated at intensities significantly >5.0 W cm^{-2}. Magnetic resonance observations revealed temperature increases in the brain after insonation that had caused necrosis of the entire sonicated area following interruption of the vascular supply.

In a further simulation of tissue heating by microbubbles at 1 mW cm^{-2}, Umemura et al. (2005) found that the increased absorption of ultrasound was primarily at the resonance frequency; with ultrasonic intensities of 1 W cm^{-2}, increased absorption occurred at both resonance and subharmonic frequencies. At intensities greater than 1 W cm^{-2}, ultrasound absorption was observed at two or three broadband resonance peaks. They concluded that microbubble-enhanced absorption doubled at microbubble concentrations as low as 8 bubbles mm^{-3}. *In vivo* experiments in rat kidneys at high spatial peak intensities up to 290 W cm^{-2} in the focal range increased temperature by three to five times and caused coagulative necrosis of the tissue. In another study, Klotz et al. (2010) modeled microbubble oscillations in a simulated microvascular network of the rat brain using focused ultrasound. The Pennes bioheat transfer equation was used to calculate the heat absorbed during the microbubble oscillations, and Klotz et al. reported that the temperature increased most around the bubbles and, to lesser extent, throughout the tissues. In the presence of 10^7 microbubbles mL^{-1}, the ideal insonation parameters were found to be 1.5 MHz and pressure amplitudes of 0.8–1.4 MPa.

Predominantly cavitation bio-effects

In a review of *in vitro* observations of the effects of insonation of cancer cells in the presence of microbubbles, Bai et al. (2012a) concluded that microbubble

heating at <0.2 MPa may be related to stable cavitation; at higher acoustic pressures >0.6 MPa, inertial cavitation becomes important. Use of a low-intensity insonation in the presence of microbubbles similar to that used by Wood et al. (2007, 2008), Lin et al. (2012a) found in rabbits that the growth of colorectal adenocarcinoma was inhibited; however, they hypothesized that during insonation, oscillation of the microbubble and its collapse with violent cavitation may disrupt the walls of the tumor neovasculature and so delay tumor growth.

Intravascular inertial cavitation was observed in rabbit ears by Tu et al. (2006) using focused ultrasound at 1.17 MHz and peak rarefaction pressures of 1–9 MPa (estimated intensity = 40–1,000 W cm^{-2}). Other *in vivo* studies of tumor models have centered on the anti-vascular actions of pulsed ultrasound beams at higher intensities and pressure amplitudes where the predominant effect on circulating microbubbles has been inertial cavitation. Using pulsed ultrasound, Goertz et al. (2008, 2009) insonated various murine tumors after the intravenous injection of microbubbles and found a reduction in tumor blood flow; when weekly treatments were given, the growth of the tumor was inhibited (Goertz et al. 2009). They reported that the signals emitted from the microbubbles during tumor insonation were consistent with the occurrence of inertial cavitation (Goertz et al. 2009). Cavitation was also considered to be the bio-effect leading to reduced tumor growth, tumor necrosis and decreased expression of an angiogenesis marker (CD31) (Huang et al. 2013).

Zhong et al. (2010) observed that ultrasound at a high mechanical index of 1.7 (an estimated intensity of 133 W cm^{-2}) and microbubbles inhibited hepatic metastases from a colon carcinoma in the spleen of rats. The metastases were smaller in number and size. Histology of the spleen revealed a decrease in the number of tumor cells, hemorrhage and necrosis. It was concluded that cavitation had damaged the capillaries, activated coagulation systems and induced thromboses leading to avascular regions and blockage of metastatic channels.

Using higher peak intensities (2.6 and 4.8 MPa), Liu et al. (2012) insonated a rat tumor after intravenous injection of microbubbles and described disruption of the tumor microvasculature. Therapy was accompanied by decreases in tumor temperature and tumor mean gray scale. It was believed that the vascular effects were due to cavitation; these findings were supported by additional observations by Peijing et al. (2014) in a rabbit tumor. Ultrasound at 4.3 MPa in combination with microbubbles enhanced liver ethanol ablation in rabbits and was accompanied by temporary interruption of perfusion (Liu et al. 2013a). Wang et al. (2013a) investigated the effect of focused ultrasound (mechanical index of 0.1–0.3, I_{SPTA} = 539 mW cm^{-2}) and microbubbles on the permeability of the capillaries of a rat hepatoma; Evans blue was the marker of vascular permeability. They suggested that the treatment regimen could induce intravascular cavitation, thus increasing the permeability of the neovasculature; higher-mechanical-index sonications caused more cavitation and induced greater vascular permeability.

Role of other bio-effects, chemotherapeutic and anti-angiogenic agents and anti-angiogenic genes

Other bio-effects of therapy have also been considered. After repeated daily treatments (over about 12 d) of a mouse colon adenocarcinoma in the presence of circulating microbubbles, Chin et al. (2009) found that the tumors were smaller and insonation caused no significant temperature increases. They hypothesized that it was unlikely that tumor cells or vascular endothelium was destroyed acutely during treatment, as tumor blood flow was restored after each therapy. They attributed the reduced tumor growth to an inflammatory response. After the intravenous injection of microbubbles, Burke et al. (2011) insonated (treatment time = 1 h) C6 rat glioma tumors implanted subcutaneously in mice using very short duty cycles (0.00002–0.01 s). A week after therapy, tumor necrosis and tumor growth inhibition were greatest where the longest duty cycles were used and the temperature of the tumor also increased post-therapy (an increase of 5.4°C at a duty cycle of 0.01 s). It was hypothesized that mechanical bio-effects were more important than thermal effects in the anti-vascular actions.

In another study of the breast cancer cell model in mice, microbubbles conjugated with peptides were injected and bound to tumor endothelial cell receptors (Hu et al. 2012). Insonation resulted in reduced tumor blood flow, which returned to normal within 30 min. It was hypothesized that platelet activation was the likely mechanism for flow reduction in the neovasculature.

It was reported by Goertz et al. (2012) that anti-vascular action is enhanced by using the chemotherapeutic agent docetaxel at a higher pressure amplitude (1.65 MPa), and it was believed that inertial cavitation was the major source of the anti-vascular effects. By labeling a drug-loaded (carmustine) microbubble with an antigen to vascular endothelial growth factor, Fan et al. (2013b) enhanced delivery of the chemotherapeutic agent to the tumor neovasculature. Use of the anti-angiogenic complex was studied in a rat glioma model in which the blood–brain barrier was broken down in the presence of insonation and the circulating microbubbles. Local delivery of the chemotherapeutic agent was enhanced with resultant suppression of the growth of the glioma, and the animals' survival time was increased.

Improved anti-tumor activity provided by anti-cancer drugs in the presence of ultrasound and microbubbles was also reported by Rapoport et al. (2007) (2.0 W cm^{-2}), Burke and Price (2010) (undefined chemotherapeutic agent and ultrasound intensities) and Lin et al. (2012b) (0.6 MPa). Anti-tumor activity was also superior when metronomic chemotherapy was combined with ultrasound and microbubbles at an ultrasound pressure amplitude of 1.65 MPa (Todorova et al. 2013).

Zhang et al. (2014) conjugated an anti-angiogenic drug (Endostar) with microbubbles and retro-orbitally injected these into mice with a subcutaneous human colon cancer before insonation (238 kHz, pulsed, 0.5 MPa). They reported inhibition of tumor blood flow and delay in tumor growth related to decreased expression of vascular endothelial growth factor receptor 2 and $\alpha v\beta$-3 integrin.

In observations of a murine colorectal adenocarcinoma, neoplastic cells were implanted in the ear (Lin et al. 2012b). Polyethylene glycol-coated liposomes loaded with doxorubicin were intravenously injected, followed by intravenous microbubbles and insonation (1.0 MHz, pulsed, 2.0 W cm^{-2}). Tumor growth was significantly inhibited, and therapy was considered to have disrupted tumor blood vessels and enhanced the delivery of drug into tumor tissue; that is, the anti-vascular effect trapped the doxorubicin in the tumor. Because of the vascular damage within the tumor, Lin et al. (2012b) raised the possibility that their treatment may facilitate the release of neoplastic cells into the general circulation, leading to metastatic disease. Kang et al. (2010), however, found that although metastases from a liver tumor in rabbits still occurred, their extent was reduced after therapy with docetaxel-loaded microbubbles and ultrasound.

There is also interest in a primarily anti-vascular role of gene therapy techniques. In a murine hepatocellular carcinoma model, Nie et al. (2008) intravenously injected plasmid DNA with microbubbles and then insonated the subcutaneous tumor. Transference of an anti-angiogenic gene resulted in a significant anti-vascular effect with reduced microvessel density and tumor growth. Unlike the majority of studies in which microbubbles were injected intravenously, Duvshani-Eshet et al. (2007) used intratumoral injections of Optison to facilitate delivery of an angiogenesis-inhibiting gene; the murine prostate cancer was insonated at 2.0 W cm^{-2}, and tumor growth was inhibited especially when weekly treatments were given over 4 wk. Many anti-vascular effects are mediated through effects on the endothelial cells of the tumor neovasculature. *In vitro* culture studies by Al-Mahrouki et al. (2012) indicated that microbubbles stimulated at 0.57 MPa upregulated the genes involved in apoptosis pathways.

Additional comments

The combination of the use of microbubbles for both anti-vascular therapy and vascular imaging is an important innovation, as such a theranostic agent exploits the use of ultrasound imaging for monitoring the success of anti-cancer therapy. Targeting the neovascular cell compartment of a tumor with low-intensity ultrasound in the presence of circulating microbubbles of ultrasound contrast agent consistently resulted in loss of tumor vascular perfusion. As a result, the neoplastic cell compartment within the avascular regions underwent liquefactive necrosis with a resultant decrease in tumor volume and an increase in survival times of the laboratory animals. The velocity of blood flow in the tumor neovasculature is slower than that in the vessels of the normal contiguous tissues, thus explaining why the bio-effects resulting from the interaction between ultrasound and a microbubble are so much greater within a neoplasm and why the circulation of the adjacent normal tissues appears unaffected. Thus, the therapy technique accurately targets the neovasculature of the tumor while sparing the normal blood vessels in the adjacent healthy tissues.

In the anti-vascular treatment of a neoplasm it is essential to deliver sufficient energy to the circulating microbubbles within the lumens of the tumor neovasculature. The microbubbles provide a mechanism for delivering the acoustic energy at sites contiguous with the endothelial cells lining the neovasculature, resulting in their disruption. Both thermal and cavitation effects have been implicated as biophysical mechanisms of interaction. Those studies using continuous wave ultrasound have emphasized thermal bio-effects, whereas the pulsed ultrasound observations have emphasized cavitation. It is difficult to separate the two effects. In all likelihood, both effects are likely to play a role, although by varying the nature of sonication conditions, one or the other mechanism may dominate. For example, low intensities and long tone bursts or continuous wave ultrasound may emphasize microbubble oscillations for long intervals and thus lead to significant heating effects. Higher intensities with shorter pulses may, on the other hand, emphasize bubble collapse and thus inertial cavitation. In addition, other non-thermal effects including microshear associated with microbubble oscillations, radiation pressure and sonochemical reactions may also play a role, although to date the evidence for these mechanisms is limited.

Cancer cell death is a secondary effect of anti-vascular ultrasound: it has both benefits and limitations. The benefit is that the effect is generic and not specific to any tumor type. Further, it does not require treatment of individual cancer cells, because the survival of several thousand cells depends on an individual blood vessel; disrupting a few blood vessels could trigger cell death in

many cancer cells. Anti-vascular ultrasound requires access only to the surface of the endothelial cells, unlike anti-vascular drugs that need to penetrate the cells to affect their cytoskeleton. Also, compared with high-intensity focused ultrasound, the anti-vascular ultrasound instruments are likely to be less costly, simpler to design and safer to use in clinical settings. In anti-vascular ultrasound, the insonating beam in unfocused, so that the entire neoplasm can be treated directly without the need to "paint" the lesion with successive small regions of treatment. A limitation of anti-vascular ultrasound is that susceptible tumor neovasculature has to be present for the therapy to be effective.

Future studies could be aimed at further investigating the potential for inciting an intratumoral immune response (Hunt et al. 2014) and enhancing chemotherapeutic retention. After anti-vascular ultrasound therapy of murine melanomas, Hunt et al. (2014) described a lymphocyte-mediated inflammation characterized by the presence of T lymphocytes within the tumors, which raises the possibility of the induction of a systemic post-therapy immune response against the cancer cells. In post-therapy MR observations of the melanomas, Hunt et al. (2014) found that washout of the MR contrast agent, gadolinium, was decreased and it was retained within the tumor, thus supporting the work of Goertz et al. (2012) and illustrating the potential role of anti-vascular ultrasound in trapping a simultaneously administered therapeutic agent within the tumor (Goertz et al. 2012).

The anti-vascular effects on the tumor neovasculature are potent, but there remains, however, a need for additional experiments to optimize the bio-effects; the anti-vascular effects should be maximized while continuing to minimize the collateral damage in the adjacent normal tissues. The differences in mechanisms of interaction for different sonication intensities also need to be investigated.

CONCLUSIONS

Sonodynamic therapy, ultrasound-mediated chemotherapy and gene delivery and anti-vascular ultrasound therapy, all of which use low-intensity ultrasound, consistently produced bio-effects that resulted in the death of cancer cells. Low-intensity applications of ultrasound are believed to be tolerable and non-toxic, can easily be applied to a tumor and require relatively inexpensive equipment. It is probable that more than a single bio-effect resulted in the efficacy of a therapy, although the importance of thermal and inertial cavitation bio-effects has been established in animal tumor models. In some situations, the accessibility of the tumor to insonation is a limitation as the cancer cells may be contiguous with a gas-containing structure or bone and not easily reached by the ultrasound beam. In such clinical situations, this limitation can be overcome by the use of intracavity transducers for imaging and therapy. Furthermore, the currently designed microbubbles have a limited loading capacity to deliver therapeutic agents at the required dosages. These limitations could be overcome by an improved microbubble design so that they can carry greater payloads. Co-administration of therapeutic agents along with the microbubbles could also be exploited as a means to overcome the issue of sufficient payload.

There is a generally held assumption that the agents used with ultrasound and microbubbles are not themselves directly affected by the insonation. In the presence of microbubble collapse and cavitation, sonochemical effects of ultrasound may also occur (Verrall and Sehgal 1988). Thus it remains to be learned whether injected agents including chemotherapeutics, genes or other sonosensitizers are not directly altered by ultrasound in the presence of microbubbles; the lack of any significant direct insonation effect on these agents could potentially accelerate their clinical acceptance and introduction. Further, the underlying mechanisms of action and transport of the agents from the tumor neovasculature to their site of action in the extravascular space of the tumor could be further explored. Finally, because the neovasculature plays such a crucial role in delivery of the agents, the *in vitro* cellular studies that are commonly performed by direct insonation should also, in the future, take into consideration the role of tumor neovasculature.

The use of microbubbles for both therapy and vascular imaging is an important innovation, as such a theranostic agent establishes a therapeutic–diagnostic platform that can monitor the success of anti-cancer therapy. The literature contains a large amount of data on the effects of low-intensity ultrasound therapy on cancer cells and mostly subcutaneously located tumor models in mice and rats. Future animal cancer trials should include longitudinal studies in which repeated treatments are given over time, as these would mimic the likely clinical treatment regimens. There is a paucity of data, however, on the value of each of these therapies in naturally occurring cancers and in larger mammals; if the results of such future investigations were encouraging, they could promptly be applied in a clinical trial.

REFERENCES

Abe H, Kuroki M, Tachibana K, Li T, Awasthi A, Ueno A, Matsumoto H, Imakiire T, Yamauchi Y, Yamada H, Ariyoshi A, Kuroki M. Targeted sonodynamic therapy of cancer using a photosensitizer conjugated with antibody against carcinoembryonic antigen. Anticancer Res 2002;22:1575–1580.

Al-Mahrouki AA, Karshafian R, Giles A, Czarnota GJ. Bioeffects of ultrasound-stimulated microbubbles on endothelial cells: Gene

expression changes associated with radiation enhancement in vitro. Ultrasound Med Biol 2012;38:1958–1969.
Anderson CR, Hu X, Zhang H, Tlaxca J, Declèves AE, Houghtaling R, Sharma K, Lawrence M, Ferrara KW, Rychak JJ. Ultrasound molecular imaging of tumor angiogenesis with an integrin targeted microbubble contrast agent. Invest Radiol 2011;46:215–224.
Aryal M, Vykhodtseva N, Zhang YZ, Park J, McDannold N. Multiple treatments with liposomal doxorubicin and ultrasound-induced disruption of blood–tumor and blood–brain barriers improve outcomes in a rat glioma model. J Control Release 2013;169:103–111.
Baker KG, Robertson VJ, Duck FA. A review of therapeutic ultrasound: Biophysical effects. Phys Ther 2001;81:1351–1358.
Bai WK, Shen E, Hu B. The induction of the apoptosis of cancer cell by sonodynamic therapy: A review. Chin J Cancer Res 2012a;24: 368–373.
Bai WK, Wu ZH, Shen E, Zhang JZ, Hu B. The improvement of liposome-mediated transfection of pEGFP DNA into human prostate cancer cells by combining low-frequency and low-energy ultrasound with microbubbles. Oncol Rep 2012b;27:475–480.
Barati AH, Mokhtari-Dizaji M, Mozdarani H, Bathaie SZ, Hassan ZM. Treatment of murine tumors using dual-frequency ultrasound in an experimental in vivo model. Ultrasound Med Biol 2009;35: 756–763.
Barati AH, Mokhtari-Dizaji M. Ultrasound dose fractionation in sonodynamic therapy. Ultrasound Med Biol 2010;36:880–887.
Bernard V, Fojt L, Skorpíková J, Mornstein V. Determination of free cisplatin in medium by differential pulse polarography after ultrasound and cisplatin treatment of a cancer cell culture. Indian J Biochem Biophys 2011;48:59–62.
Bernard V, Mornstein V, Škorpíková J, Jaroš J. Ultrasound and cisplatin combined treatment of human melanoma cells A375—The study of sonodynamic therapy. Ultrasound Med Biol 2012;38:1205–1211.
Bunte RM, Ansaloni S, Sehgal CM, Lee WM, Wood AK. Histopathological observations of the antivascular effects of physiotherapy ultrasound on a murine neoplasm. Ultrasound Med Biol 2006;32: 453–461.
Burgess A, Hynynen K. Drug delivery across the blood–brain barrier using focused ultrasound. Expert Opin Drug Deliv 2014;11:711–721.
Burke CW, Price RJ. Contrast ultrasound targeted treatment of gliomas in mice via drug-bearing nanoparticle delivery and micro-vascular ablation. J Vis Exp 2010;46:e2145.
Burke CW, Klibanov AL, Sheehan JP, Price RJ. Inhibition of glioma growth by microbubble activation in a subcutaneous model using low duty cycle ultrasound without significant heating. J Neurosurg 2011;114:1654–1661.
Carson AR, McTiernan CF, Lavery L, Hodnick A, Grata M, Leng X, Wang J, Chen X, Modzelewski RA, Villanueva FS. Gene therapy of carcinoma using ultrasound-targeted microbubble destruction. Ultrasound Med Biol 2011;37:393–402.
Carson AR, McTiernan CF, Lavery L, Grata M, Leng X, Wang J, Chen X, Villanueva FS. Ultrasound-targeted microbubble destruction to deliver siRNA cancer therapy. Cancer Res 2012;72: 6191–6199.
Chang S, Guo J, Sun J, Zhu S, Yan Y, Zhu Y, Li M, Wang Z, Xu RX. Targeted microbubbles for ultrasound mediated gene transfection and apoptosis induction in ovarian cancer cells. Ultrason Sonochem 2013;20:171–179.
Chen B, Zheng R, Liu D, Li B, Lin J, Zhang W. The tumor affinity of chlorin e6 and its sonodynamic effects on non-small cell lung cancer. Ultrason Sonochem 2013a;20:667–673.
Chen CC, Sheeran PS, Wu SY, Olumolade OO, Dayton PA, Konofagou EE. Targeted drug delivery with focused ultrasound-induced blood–brain barrier opening using acoustically-activated nanodroplets. J Control Release 2013b;172:795–804.
Chen JJ, Chen JJ, Chiang CS, Hong JH, Yeh CK. Assessment of tumor vasculature for diagnostic and therapeutic applications in a mouse model in vivo using 25-MHz power Doppler imaging. Ultrasonics 2011;51:925–931.
Chen JJ, Fu SY, Chiang CS, Hong JH, Yeh CK. Characterization of tumor vasculature distributions in central and peripheral regions based on Doppler ultrasound. Med Phys 2012a;39:7490–7498.
Chen JJ, Fu SY, Chiang CS, Hong JH, Yeh CK. A preclinical study to explore vasculature differences between primary and recurrent tumors using ultrasound Doppler imaging. Ultrasound Med Biol 2013c;39:860–869.
Chen Z, Li J, Song X, Wang Z, Yue W. Use of a novel sonosensitizer in sonodynamic therapy of U251 glioma cells in vitro. Exp Ther Med 2012b;3:273–278.
Chen H, Zhou X, Gao Y, Zheng B, Tang F, Huang J. Recent progress in development of new sonosensitizers for sonodynamic cancer therapy. Drug Discov Today 2014;19:502–509.
Chin CT, Raju BI, Shevchenko T, Klibanov AL. Control and reversal of tumor growth by ultrasound activated microbubbles. Proc IEEE Int Ultrason Symp 2009;77–80.
Chumakova OV, Liopo AV, Evers BM, Esenaliev RO. Effect of 5-fluorouracil, Optison and ultrasound on MCF-7 cell viability. Ultrasound Med Biol 2006;32:751–758.
Cochran MC, Eisenbrey J, Ouma RO, Soulen M, Wheatley MA. Doxorubicin and paclitaxel loaded microbubbles for ultrasound triggered drug delivery. Int J Pharm 2011;414:161–170.
Cool SK, Geers B, Roels S, Stremersch S, Vanderperren K, Saunders JH, De Smedt SC, Demeester J, Sanders NN. Coupling of drug containing liposomes to microbubbles improves ultrasound triggered drug delivery in mice. J Control Release 2013;172:885–893.
Cosgrove D. Ultrasound contrast agents: An overview. Eur J Radiol 2006;60:324–330.
Derieppe M, Yudina A, Lepetit-Coiffé M, de Senneville BD, Bos C, Moonen C. Real-time assessment of ultrasound-mediated drug delivery using fibered confocal fluorescence microscopy. Mol Imaging Biol 2013;15:3–11.
Duvshani-Eshet M, Benny O, Morgenstern A, Machluf M. Therapeutic ultrasound facilitates antiangiogenic gene delivery and inhibits prostate tumor growth. Mol Cancer Ther 2007;6:2371–2382.
Escoffre JM, Mannaris C, Geers B, Novell A, Lentacker I, Averkiou M, Bouakaz A. Doxorubicin liposome-loaded microbubbles for contrast imaging and ultrasound-triggered drug delivery. IEEE Trans Ultrason Ferroelectr Freq Control 2013;60:78–87.
Escoffre JM, Piron J, Novell A, Bouakaz A. Doxorubicin delivery into tumor cells with ultrasound and microbubbles. Mol Pharm 2011;8: 799–806.
Fan CH, Ting CY, Lin HJ, Wang CH, Liu HL, Yen TC, Yeh CK. SPIO-conjugated, doxorubicin-loaded microbubbles for concurrent MRI and focused-ultrasound enhanced brain-tumor drug delivery. Biomaterials 2013a;34:3706–3715.
Fan CH, Ting CY, Liu HL, Huang CY, Hsieh HY, Yen TC, Wei KC, Yeh CK. Antiangiogenic-targeting drug-loaded microbubbles combined with focused ultrasound for glioma treatment. Biomaterials 2013b;34:2142–2155.
Feril LB, Ogawa R, Tachibana K, Kondo T. Optimized ultrasound-mediated gene transfection in cancer cells. Cancer Sci 2006;97: 1111–1114.
Feril LB, Tachibana K, Kondo T, Campbell PA. Sonodynamic therapy. In: Frenkel V, (ed). Therapeutic ultrasound mechanisms to applications. New York: Nova Sciences; 2011. p. 279–295.
Feril LB, Tachibana K. Use of ultrasound in drug delivery systems: Emphasis on experimental methodology and mechanisms. Int J Hyperthermia 2012;28:282–289.
Ferrara KW, Borden MA, Zhang H. Lipid-shelled vehicles: Engineering for ultrasound molecular imaging and drug delivery. Acc Chem Res 2009;42:881–892.
Fokong S, Theek B, Wu Z, Koczera P, Appold L, Jorge S, Resch-Genger U, van Zandvoort M, Storm G, Kiessling F, Lammers T. Image-guided, targeted and triggered drug delivery to tumors using polymer-based microbubbles. J Control Release 2012;163:75–81.
Folkman J. Angiogenesis. In: Braunwald E, Fauci AS, Kasper DL, Hauser SL, Longo DL, Jameson JL, (eds). Harrison's textbook of internal medicine. New York: McGraw-Hill; 2001. p. 517–530.
Fujii H, Matkar P, Liao C, Rudenko D, Lee PJ, Kuliszewski MA, Prud'homme GJ, Leong-Poi H. Optimization of ultrasound-mediated anti-angiogenic cancer gene therapy. Mol Ther Nucleic Acids 2013;2:e94 [Epub 2013 May 21.].

Gao ZG, Fain HD, Rapoport N. Controlled and targeted tumor chemotherapy by micellar-encapsulated drug and ultrasound. J Control Release 2005;102:203–222.
Gao HJ, Zhang WM, Wang XH, Zheng RN. Adriamycin enhances the sonodynamic effect of chlorin e6 against the proliferation of human breast cancer MDA-MB-231 cells in vitro. J South Med Univ 2010; 30:2291–2294.
Gao Z, Zheng J, Yang B, Wang Z, Fan H, Lv Y, Li H, Jia L, Cao W. Sonodynamic therapy inhibits angiogenesis and tumor growth in a xenograft mouse model. Cancer Lett 2013;335:93–99.
Geers B, Lentacker I, Sanders NN, Demeester J, Meairs S, De Smedt SC. Self-assembled liposome-loaded microbubbles: The missing link for safe and efficient ultrasound triggered drug-delivery. J Control Release 2011;152:249–256.
Geis NA, Katus HA, Bekeredjian R. Microbubbles as a vehicle for gene and drug delivery: Current clinical implications and future perspectives. Curr Pharm Des 2012;18:2166–2183.
Goertz DE, Karshafian R, Hynynen K. Antivascular effects of pulsed low intensity ultrasound and microbubbles in mouse tumors. Proc IEEE Int Ultrason Symp 2008;670–673.
Goertz DE, Karshafian R, Hynynen K. Investigating the effects of pulsed low intensity ultrasound and microbubbles in mouse tumors. Proc IEEE Int Ultrason Symp Proc 2009;89–92.
Goertz DE, Todorova M, Mortazavi O, Agache V, Chen B, Karshafian R, Hynynen K. Antitumor effects of combining docetaxel (taxotere) with the antivascular action of ultrasound stimulated microbubbles. PLoS One 2012;7:e52307.
Goertz DE, Yu JL, Kerbel RS, Burns PN, Foster FS. High-frequency Doppler ultrasound monitors the effects of antivascular therapy on tumor blood flow. Cancer Res 2002;62:6371–6375.
Haag P, Frauscher F, Gradl J, Seitz A, Schäfer G, Lindner JR, Klibanov AL, Bartsch G, Klocker H, Eder IE. Microbubble-enhanced ultrasound to deliver an antisense oligodeoxynucleotide targeting the human androgen receptor into prostate tumours. J Steroid Biochem Mol Biol 2006;102:103–113.
Hachimine K, Shibaguchi H, Kuroki M, Yamada H, Kinugasa T, Nakae Y, Asano R, Sakata I, Yamashita Y, Shirakusa T, Kuroki M. Sonodynamic therapy of cancer using a novel porphyrin derivative, DCPH–P–Na(I), which is devoid of photosensitivity. Cancer Sci 2007;98:916–920.
Hassan MA, Furusawa Y, Minemura M, Rapoport N, Sugiyama T, Kondo T. Ultrasound-induced new cellular mechanism involved in drug resistance. PLoS One 2012;7:e48291.
Hauser J, Ellisman M, Steinau HU, Stefan E, Dudda M, Hauser M. Ultrasound enhanced endocytotic activity of human fibroblasts. Ultrasound Med Biol 2009;35:2084–2092.
Heath CH, Sorace A, Knowles J, Rosenthal E, Hoyt K. Microbubble therapy enhances anti-tumor properties of cisplatin and cetuximab in vitro and in vivo. Otolaryngol Head Neck Surg 2012;146: 938–945.
Hu X, Kheirolomoom A, Mahakian LM, Beegle JR, Kruse DE, Lam KS, Ferrara KW. Insonation of targeted microbubbles produces regions of reduced blood flow within tumor vasculature. Invest Radiol 2012;47:398–405.
Huang P, You X, Pan M, Li S, Zhang Y, Zhao Y, Wang M, Hong Y, Pu Z, Chen L, Yang G, Guo Y. A novel therapeutic strategy using ultrasound mediated microbubbles destruction to treat colon cancer in a mouse model. Cancer Lett 2013;335:183–190.
Hunt SJ, Gade T, Soulen MC, Pickup S, Sehgal CM. Antivascular ultrasound therapy: MR validation and activation of immune response in murine melanoma. J Ultrasound Med 2015;34:275–287.
Husseini GA, Pitt WG. Ultrasonic-activated micellar drug delivery for cancer treatment. J Pharm Sci 2009;98:795–811.
Hyvelin JM, Tardy I, Arbogast C, Costa M, Emmel P, Helbert A, Theraulaz M, Nunn AD, Tranquart F. Use of ultrasound contrast agent microbubbles in preclinical research: Recommendations for small animal imaging. Invest Radiol 2013;48:570–583.
Ibsen S, Benchimol M, Simberg D, Esener S. Ultrasound mediated localized drug delivery. Adv Exp Med Biol 2012;733:145–153.
Ibsen S, Schutt CE, Esener S. Microbubble-mediated ultrasound therapy: A review of its potential in cancer treatment. Drug Des Devel Ther 2013;7:375–388.
Jeong EJ, Seo SJ, Ahn YJ, Choi KH, Kim KH, Kim JK. Sonodynamically induced antitumor effects of 5-aminolevulinic acid and fractionated ultrasound irradiation in an orthotopic rat glioma model. Ultrasound Med Biol 2012;38:2143–2150.
Jin ZH, Miyoshi N, Ishiguro K, Umemura S, Kawabata K, Yumita N, Sakata I, Takaoka K, Udagawa T, Nakajima S, Tajiri H, Ueda K, Fukuda M, Kumakiri M. Combination effect of photodynamic and sonodynamic therapy on experimental skin squamous cell carcinoma in C3 H/HeN mice. J Dermatol 2000;27:294–306.
Kang J, Wu X, Wang Z, Ran H, Xu C, Wu J, Wang Z, Zhang Y. Antitumor effect of docetaxel-loaded lipid microbubbles combined with ultrasound-targeted microbubble activation on VX2 rabbit liver tumors. J Ultrasound Med 2010;29:61–70.
Kang ST, Yeh CK. Ultrasound microbubble contrast agents for diagnostic and therapeutic applications: Current status and future design. Chang Gung Med J 2012;35:125–139.
Kovacs Z, Werner B, Rassi A, Sass JO, Martin-Fiori E, Bernasconi M. Prolonged survival upon ultrasound-enhanced doxorubicin delivery in two syngenic glioblastoma mouse models. J Control Release 2014;187:74–82.
Klotz AR, Lindvere L, Stefanovic B, Hynynen K. Temperature change near microbubbles within a capillary network during focused ultrasound. Phys Med Biol 2010;55:1549–1561.
Kuroki M, Hachimine K, Abe H, Shibaguchi H, Kuroki M, Maekawa S, Yanagisawa J, Kinugasa T, Tanaka T, Yamashita Y. Sonodynamic therapy of cancer using novel sonosensitizers. Anticancer Res 2007;27:3673–3677.
Lentacker I, Geers B, Demeester J, De Smedt SC, Sanders NN. Design and evaluation of doxorubicin-containing microbubbles for ultrasound-triggered doxorubicin delivery: Cytotoxicity and mechanisms involved. Mol Ther 2010;18:101–108.
Levenback BJ, Sehgal CM, Wood AK. Modeling of thermal effects in antivascular ultrasound therapy. J Acoust Soc Am 2012;131: 540–549.
Li F, Jin L, Wang H, Wei F, Bai M, Shi Q, Du L. The dual effect of ultrasound-targeted microbubble destruction in mediating recombinant adeno-associated virus delivery in renal cell carcinoma: Transfection enhancement and tumor inhibition. J Gene Med 2014;16: 28–39.
Li H, Fan H, Wang Z, Zheng J, Cao W. Potentiation of scutellarin on human tongue carcinoma xenograft by low-intensity ultrasound. PLoS One 2013;8:e59473.
Li P, Zheng Y, Ran H, Tan J, Lin Y, Zhang Q, Ren J, Wang Z. Ultrasound triggered drug release from 10-hydroxycamptothecin-loaded phospholipid microbubbles for targeted tumor therapy in mice. J Control Release 2012a;162:349–354.
Li XH, Zhou P, Wang LH, Tian SM, Qian Y, Chen LR, Zhang P. The targeted gene (KDRP-CD/TK) therapy of breast cancer mediated by SonoVue and ultrasound irradiation in vitro. Ultrasonics 2012b;52: 186–191.
Li Y, Wang P, Zhao P, Zhu S, Wang X, Liu Q. Apoptosis induced by sonodynamic treatment by protoporphyrin IX on MDA-MB-231 cells. Ultrasonics 2012c;52:490–496.
Liang HD, Tang J, Halliwell M. Sonoporation, drug delivery, and gene therapy. Proc Inst Mech Eng H 2010;224:343–361.
Liang L, Xie S, Jiang L, Jin H, Li S, Liu J. The Combined effects of hematoporphyrin monomethyl ether-SDT and doxorubicin on the proliferation of QBC939 cell lines. Ultrasound Med Biol 2013;39: 146–160.
Liao AH, Li YK, Lee WJ, Wu MF, Liu HL, Kuo ML. Estimating the delivery efficiency of drug-loaded microbubbles in cancer cells with ultrasound and bioluminescence imaging. Ultrasound Med Biol 2012a;38:1938–1948.
Liao AH, Liu HL, Su CH, Hua MY, Yang HW, Weng YT, Hsu PH, Huang SM, Wu SY, Wang HE, Yen TC, Li PC. Paramagnetic perfluorocarbon-filled albumin–(Gd-DTPA) microbubbles for the induction of focused-ultrasound-induced blood–brain barrier opening and concurrent MR and ultrasound imaging. Phys Med Biol 2012b;57:2787–2802.
Lim AK, Patel N, Eckersley RJ, Taylor-Robinson SD, Cosgrove DO, Blomley MJ. Evidence for spleen-specific uptake of a microbubble

contrast agent: A quantitative study in healthy volunteers. Radiology 2004;231:785–788.
Lin CY, Li JR, Tseng HC, Wu MF, Lin WL. Enhancement of focused ultrasound with microbubbles on the treatments of anticancer nanodrug in mouse tumors. Nanomedicine 2012a;8:900–907.
Lin CY, Tseng HC, Shiu HR, Wu MF, Chou CY, Lin WL. Ultrasound sonication with microbubbles disrupts blood vessels and enhances tumor treatments of anticancer nanodrug. Int J Nanomed 2012b;7: 2143–2152.
Lionetti V, Paddeu S. Toward ultrasound molecular imaging. In: Paradossi G, Pellegretti P, Trucco A, (eds). Ultrasound contrast agents: Targeting and processing methods for theranostics. Berlin: Springer; 2010. p. 1.
Liu GJ, Moriyasu F, Hirokawa T, Rexiati M, Yamada M, Imai Y. Optical microscopic findings of the behavior of perflubutane microbubbles outside and inside Kupffer cells during diagnostic ultrasound examination. Invest Radiol 2008a;43:829–836.
Liu HL, Fan CH, Ting CY, Yeh CK. Combining microbubbles and ultrasound for drug delivery to brain tumors: Current progress and overview. Theranostics 2014;4:432–444.
Liu HL, Hua MY, Chen PY, Chu PC, Pan CH, Yang HW, Huang CY, Wang JJ, Yen TC, Wei KC. Blood–brain barrier disruption with focused ultrasound enhances delivery of chemotherapeutic drugs for glioblastoma treatment. Radiology 2010;255:415–425.
Liu Q, Li X, Xiao L, Wang P, Wang X, Tang W. Sonodynamically induced antitumor effect of hematoporphyrin on hepatoma 22. Ultrason Sonochem 2008b;15:943–948.
Liu Q, Wang X, Wang P, Qi H, Zhang K, Xiao L. Sonodynamic effects of protoporphyrin IX disodium salt on isolated sarcoma 180 cells. Ultrasonics 2006a;45:56–60.
Liu Q, Wang X, Wang P, Xiao L. Sonodynamic antitumor effect of protoporphyrin IX disodium salt on S180 solid tumor. Chemotherapy 2007a;53:429–436.
Liu Q, Wang X, Wang P, Xiao L, Hao Q. Comparison between sonodynamic effect with protoporphyrin IX and hematoporphyrin on sarcoma 180. Cancer Chemother Pharmacol 2007b;60:671–680.
Liu Q, Zhao H, Wu S, Zhao X, Zhong Y, Li L, Liu Z. Impact of microbubble-enhanced ultrasound on liver ethanol ablation. Ultrasound Med Biol 2013a;39:1039–1046.
Liu Y, Miyoshi H, Nakamura M. Encapsulated ultrasound microbubbles: Therapeutic application in drug/gene delivery. J Control Release 2006b;114:89–99.
Liu YN, Khangura J, Xie A, Belcik JT, Qi Y, Davidson BP, Zhao Y, Kim S, Inaba Y, Lindner JR. Renal retention of lipid microbubbles: A potential mechanism for flank discomfort during ultrasound contrast administration. J Am Soc Echocardiogr 2013b;26: 1474–1481.
Liu Z, Gao S, Zhao Y, Li P, Liu J, Li P, Tan K, Xie F. Disruption of tumor neovasculature by microbubble enhanced ultrasound: A potential new physical therapy of anti-angiogenesis. Ultrasound Med Biol 2012;38:253–261.
Lu CT, Zhao YZ, Wu Y, Tian XQ, Li WF, Huang PT, Li XK, Sun CZ, Zhang L. Experiment on enhancing antitumor effect of intravenous epirubicin hydrochloride by acoustic cavitation in situ combined with phospholipid-based microbubbles. Cancer Chemother Pharmacol 2011;68:343–348.
Lv Y, Fang M, Zheng J, Yang B, Li H, Xiuzigao Z, Song W, Chen Y, Cao W. Low-intensity ultrasound combined with 5-aminolevulinic acid administration in the treatment of human tongue squamous carcinoma. Cell Physiol Biochem 2012;30:321–333.
Mason RP, Zhao D, Liu L, Trawick ML, Pinney KG. A perspective on vascular disrupting agents that interact with tubulin: Preclinical tumor imaging and biological assessment. Integr Biol (Camb) 2011; 3:375–387.
Matsuo M, Yamaguchi K, Feril LB Jr, Endo H, Ogawa K, Tachibana K, Nakayama J. Synergistic inhibition of malignant melanoma proliferation by melphalan combined with ultrasound and microbubbles. Ultrason Sonochem 2011;18:1218–1224.
Mayer CR, Geis NA, Katus HA, Bekeredjian R. Ultrasound targeted microbubble destruction for drug and gene delivery. Expert Opin Drug Deliv 2008;5:1121–1138.
McDannold NJ, Vykhodtseva NI, Hynynen K. Microbubble contrast agent with focused ultrasound to create brain lesions at low power levels: MR imaging and histologic study in rabbits. Radiology 2006;241:95–106.
Meijering BD, Juffermans LJ, van Wamel A, Henning RH, Zuhorn IS, Emmer M, Versteilen AM, Paulus WJ, van Gilst WH, Kooiman K, de Jong N, Musters RJ, Deelman LE, Kamp O. Ultrasound and microbubble-targeted delivery of macromolecules is regulated by induction of endocytosis and pore formation. Circ Res 2009;104: 679–687.
Misík V, Riesz P. Free radical intermediates in sonodynamic therapy. Ann NY Acad Sci 2000;899:335–348.
Nie F, Xu HX, Lu MD, Wang Y, Tang Q. Anti-angiogenic gene therapy for hepatocellular carcinoma mediated by microbubble-enhanced ultrasound exposure: An in vivo experimental study. J Drug Target 2008;16:389–395.
Ninomiya K, Ogino C, Oshima S, Sonoke S, Kuroda S, Shimizu N. Targeted sonodynamic therapy using protein-modified TiO2 nanoparticles. Ultrason Sonochem 2012;19:607–614.
Ninomiya K, Noda K, Ogino C, Kuroda S, Shimizu N. Enhanced OH radical generation by dual-frequency ultrasound with TiO2 nanoparticles: Its application to targeted sonodynamic therapy. Ultrason Sonochem 2014;21:289–294.
Niu C, Wang Z, Lu G, Krupka TM, Sun Y, You Y, Song W, Ran H, Li P, Zheng Y. Doxorubicin loaded superparamagnetic PLGA-iron oxide multifunctional microbubbles for dual-mode US/MR imaging and therapy of metastasis in lymph nodes. Biomaterials 2013;34: 2307–2317.
Nomikou N, Li YS, McHale AP. Ultrasound-enhanced drug dispersion through solid tumours and its possible role in aiding ultrasound-targeted cancer chemotherapy. Cancer Lett 2010;288:94–98.
Nomikou N, McHale AP. Exploiting ultrasound-mediated effects in delivering targeted, site-specific cancer therapy. Cancer Lett 2010; 296:133–143.
Ohmura T, Fukushima T, Shibaguchi H, Yoshizawa S, Inoue T, Kuroki M, Sasaki K, Umemura S. Sonodynamic therapy with 5-aminolevulinic acid and focused ultrasound for deep-seated intracranial glioma in rat. Anticancer Res 2011;31:2527–2533.
Owen J, Pankhurst Q, Stride E. Magnetic targeting and ultrasound mediated drug delivery: Benefits, limitations and combination. Int J Hyperthermia 2012;28:362–373.
Park EJ, Zhang YZ, Vykhodtseva N, McDannold N. Ultrasound-mediated blood–brain/blood–tumor barrier disruption improves outcomes with trastuzumab in a breast cancer brain metastasis model. J Control Release 2012;163:277–284.
Peijing L, Mei Z, Yali X, Yang Z, Shunji G, Gao YG. Impact of microbubble enhanced, pulsed, focused ultrasound on tumor circulation of subcutaneous VX2 cancer. Chin Med J 2014;127:2605–2611.
Perini R, Choe R, Yodh AG, Sehgal C, Divgi CR, Rosen MA. Non-invasive assessment of tumor neovasculature: Techniques and clinical applications. Cancer Metastasis Rev 2008;27:615–630.
Peyman SA, Abou-Saleh RH, Evans SD. Research Spotlight: Microbubbles for therapeutic delivery. Ther Deliv 2013;4:539–542.
Preston RC. Hydrophone-based measurements on a specific acoustic pulse: Part 1. Field characterization. In: Preston RC, (ed). Output measurements for medical ultrasound. London: Springer-Verlag; 1991.
Rapoport N. Ultrasound-mediated micellar drug delivery. Int J Hyperthermia 2012;28:374–385.
Rapoport N, Gao Z, Kennedy A. Multifunctional nanoparticles for combining ultrasonic tumor imaging and targeted chemotherapy. J Natl Cancer Inst 2007;99:1095–1106.
Rapoport NY, Kennedy AM, Shea JE, Scaife CL, Nam KH. Controlled and targeted tumor chemotherapy by ultrasound-activated nanoemulsions/microbubbles. J Control Release 2009;138:268–276.
Razansky D, Einziger PD, Adam DR. Enhanced heat deposition using ultrasound contrast agent–modeling and experimental observations. IEEE Trans Ultrason Ferroelectr Freq Control 2006;53:137–147.
Ren ST, Liao YR, Kang XN, Li YP, Zhang H, Ai H, Sun Q, Jing J, Zhao XH, Tan LF, Shen XL, Wang B. The antitumor effect of a new docetaxel-loaded microbubble combined with low-frequency

ultrasound in vitro: Preparation and parameter analysis. Pharm Res 2013;30:1574–1585.
Rosenthal I, Sostaric JZ, Riesz P. Sonodynamic therapy—A review of the synergistic effects of drugs and ultrasound. Ultrason Sonochem 2004;11:349–363.
Sakakima Y, Hayashi S, Yagi Y, Hayakawa A, Tachibana K, Nakao A. Gene therapy for hepatocellular carcinoma using sonoporation enhanced by contrast agents. Cancer Gene Ther 2005;12:884–889.
Samiotaki G, Konofagou EE. Dependence of the reversibility of focused-ultrasound-induced blood–brain barrier opening on pressure and pulse length in vivo. IEEE Trans Ultrason Ferroelectr Freq Control 2013;60:2257–2265.
Sazgarnia A, Shanei A, Meibodi NT, Eshghi H, Nassirli H. A novel nanosonosensitizer for sonodynamic therapy: In vivo study on a colon tumor model. J Ultrasound Med 2011;30:1321–1329.
Schroeder A, Honen R, Turjeman K, Gabizon A, Kost J, Barenholz Y. Ultrasound triggered release of cisplatin from liposomes in murine tumors. J Control Release 2009a;137:63–68.
Schroeder A, Kost J, Barenholz Y. Ultrasound, liposomes, and drug delivery: principles for using ultrasound to control the release of drugs from liposomes. Chem Phys Lipids 2009b;162:1–16.
Sehgal CM, Cary TW, Arger PH, Wood AKW. Delta-projection imaging on contrast-enhanced ultrasound to quantify tumor microvasculature and perfusion. Acad Radiol 2009;16:71–78.
Shanei A, Sazgarnia A, Tayyebi Meibodi N, Eshghi H, Hassanzadeh-Khayyat M, Esmaily H, Attaran Kakhki N. Sonodynamic therapy using protoporphyrin IX conjugated to gold nanoparticles: An in vivo study on a colon tumor model. Iran J Basic Med Sci 2012;15:759–767.
Shi H, Liu Q, Qin X, Wang P, Wang X. Pharmacokinetic study of a novel sonosensitizer chlorin-e6 and its sonodynamic anti-cancer activity in hepatoma-22 tumor-bearing mice. Biopharm Drug Dispos 2011;32:319–332.
Shibaguchi H, Tsuru H, Kuroki M, Kuroki M. Sonodynamic cancer therapy: A non-invasive and repeatable approach using low-intensity ultrasound with a sonosensitizer. Anticancer Res 2011;31:2425–2429.
Siemann DW. Tumor vasculature: A target for anticancer therapies. In: Siemann DW, (ed). Vascular-targeted therapies in oncology. Chichester: Wiley; 2006. p. 1–8.
Sirsi SR, Borden MA. Advances in ultrasound mediated gene therapy using microbubble contrast agents. Theranostics 2012;2:1208–1222.
Sirsi SR, Hernandez SL, Zielinski L, Blomback H, Koubaa A, Synder M, Homma S, Kandel JJ, Yamashiro DJ, Borden MA. Polyplex-microbubble hybrids for ultrasound-guided plasmid DNA delivery to solid tumors. J Control Release 2012;157:224–234.
Sorace AG, Warram JM, Umphrey H, Hoyt K. Microbubble-mediated ultrasonic techniques for improved chemotherapeutic delivery in cancer. J Drug Target 2012;20:43–54.
Staples BJ, Pitt WG, Roeder BL, Husseini GA, Rajeev D, Schaalje GB. Distribution of doxorubicin in rats undergoing ultrasonic drug delivery. J Pharm Sci 2010;99:3122–3131.
Stride EP, Coussios CC. Cavitation and contrast: The use of bubbles in ultrasound imaging and therapy. Proc Inst Mech Eng H 2010;224:171–191.
Su X, Li Y, Wang P, Wang X, Liu Q. Protoporphyrin IX-mediated sonodynamic action induces apoptosis of K562 cells. Ultrasonics 2014;54:275–284.
Su X, Wang P, Wang X, Cao B, Li L, Liu Q. Apoptosis of U937 cells induced by hematoporphyrin monomethyl ether-mediated sonodynamic action. Cancer Biother Radiopharm 2013a;28:207–217.
Su X, Wang P, Wang X, Guo L, Li S, Liu Q. Involvement of MAPK activation and ROS generation in human leukemia U937 cells undergoing apoptosis in response to sonodynamic therapy. Int J Radiat Biol 2013b;89:915–927.
Sugita N, Iwase Y, Yumita N, Ikeda T, Umemura S. Sonodynamically induced cell damage using rose Bengal derivative. Anticancer Res 2010;30:3361–3366.
Tang Q, He X, Liao H, He L, Wang Y, Zhou D, Ye S, Chen Q. Ultrasound microbubble contrast agent-mediated suicide gene transfection in the treatment of hepatic cancer. Oncol Lett 2012;4:970–972.
Tang W, Liu Q, Wang X, Mi N, Wang P, Zhang J. Membrane fluidity altering and enzyme inactivating in sarcoma 180 cells post the exposure to sonoactivated hematoporphyrin in vitro. Ultrasonics 2008a;48:66–73.
Tang W, Liu Q, Wang X, Wang P, Cao B, Mi N, Zhang J. Involvement of caspase 8 in apoptosis induced by ultrasound-activated hematoporphyrin in sarcoma 180 cells in vitro. J Ultrasound Med 2008b;27:645–656.
Tang W, Liu Q, Wang X, Zhang J, Wang P, Mi N. Ultrasound exposure in the presence of hematoporphyrin induced loss of membrane integral proteins and inactivity of cell proliferation associated enzymes in sarcoma 180 cells in vitro. Ultrason Sonochem 2008c;15:747–754.
Tian Z, Quan X, Xu C, Dan L, Guo H, Leung W. Hematoporphyrin monomethyl ether enhances the killing action of ultrasound on osteosarcoma in vivo. J Ultrasound Med 2009;28:1695–1702.
Ting CY, Fan CH, Liu HL, Huang CY, Hsieh HY, Yen TC, Wei KC, Yeh CK. Concurrent blood–brain barrier opening and local drug delivery using drug-carrying microbubbles and focused ultrasound for brain glioma treatment. Biomaterials 2012;33:704–712.
Tinkov S, Bekeredjian R, Winter G, Coester C. Microbubbles as ultrasound triggered drug carriers. J Pharm Sci 2009;98:1935–1961.
Tinkov S, Coester C, Serba S, Geis NA, Katus HA, Winter G, Bekeredjian R. New doxorubicin-loaded phospholipid microbubbles for targeted tumor therapy: in vivo characterization. J Control Release 2010a;148:368–372.
Tinkov S, Winter G, Coester C, Bekeredjian R. New doxorubicin-loaded phospholipid microbubbles for targeted tumor therapy: Part I. Formulation development and in vitro characterization. J Control Release 2010b;143:143–150.
Todorova M, Agache V, Mortazavi O, Chen B, Karshafian R, Hynynen K, Man S, Kerbel RS, Goertz DE. Antitumor effects of combining metronomic chemotherapy with the antivascular action of ultrasound stimulated microbubbles. Int J Cancer 2013;132:2956–2966.
Toft KG, Hustvedt SO, Hals PA, Oulie I, Uran S, Landmark K, Normann PT, Skotland T. Disposition of perfluorobutane in rats after intravenous injection of Sonazoid. Ultrasound Med Biol 2006;32:107–114.
Tomizawa M, Ebara M, Saisho H, Sakiyama S, Tagawa M. Irradiation with ultrasound of low output intensity increased chemosensitivity of subcutaneous solid tumors to an anti-cancer agent. Cancer Lett 2001;173:31–35.
Treat LH, McDannold N, Zhang Y, Vykhodtseva N, Hynynen K. Improved anti-tumor effect of liposomal doxorubicin after targeted blood–brain barrier disruption by MRI-guided focused ultrasound in rat glioma. Ultrasound Med Biol 2012;38:1716–1725.
Trendowski M. The promise of sonodynamic therapy. Cancer Metastasis Rev 2014;33:143–160.
Tserkovsky DA, Alexandrova EN, Chalau VN, Istomin YP. Effects of combined sonodynamic and photodynamic therapies with photolon on a glioma C6 tumor model. Exp Oncol 2012;34:332–335.
Tsuru H, Shibaguchi H, Kuroki M, Yamashita Y, Kuroki M. Tumor growth inhibition by sonodynamic therapy using a novel sonosensitizer. Free Radic Biol Med 2012;53:464–472.
Tu J, Hwang JH, Matula TJ, Brayman AA, Crum LA. Intravascular inertial cavitation activity detection and quantification in vivo with Optison. Ultrasound Med Biol 2006;32:1601–1609.
Umemura K, Yumita N, Nishigaki R, Umemura S. Sonodynamically induced antitumor effect of pheophorbide a. Cancer Lett 1996a;102:151–157.
Umemura S, Kawabata K, Sasaki K. In vivo acceleration of ultrasonic tissue heating by microbubble agent. IEEE Trans Ultrason Ferroelectr Freq Control 2005;52:1690–1698.
Umemura S, Kawabata K, Sasaki K, Yumita N, Umemura K, Nishigaki R. Recent advances in sonodynamic approach to cancer therapy. Ultrason Sonochem 1996b;3:S187–S191.
Umemura S, Yumita N, Nishigaki R, Umemura K. Mechanism of cell damage by ultrasound in combination with hematoporphyrin. Jpn J Cancer Res 1990;81:962–966.
Van Leenders GJLH, Beerlage HP, Th Ruijter E, de la Rosette JJMCH, van de Kaa CA. Histopathological changes associated with high intensity focused ultrasound (HIFU) treatment for localised adenocarcinoma of the prostate. J Clin Pathol 2000;53:391–394.

Vaupel P. Abnormal microvasculature and defective microcirculatory function in solid tumors. In: Siemann DW, (ed). Vascular-targeted therapies in oncology. Chichester: Wiley; 2006. p. 9–29.
Verrall RE, Sehgal CM. Sonoluminescence. In: Suslick KS, (ed). Ultrasound: Its chemical, physical and biological effects. New York: VCH; 1988. p. 227–286.
Wang DS, Panje C, Pysz MA, Paulmurugan R, Rosenberg J, Gambhir SS, Schneider M, Willmann JK. Cationic versus neutral microbubbles for ultrasound-mediated gene delivery in cancer. Radiology 2012a;264:721–732.
Wang G, Zhuo Z, Xia H, Zhang Y, He Y, Tan W, Gao Y. Investigation into the impact of diagnostic ultrasound with microbubbles on the capillary permeability of rat hepatomas. Ultrasound Med Biol 2013a;39:628–637.
Wang H, Liu Q, Zhang K, Wang P, Xue Q, Li L, Wang X. Comparison between sonodynamic and photodynamic effect on MDA-MB-231 cells. J Photochem Photobiol B 2013b;127:182–191.
Wang P, Wang XB, Liu QH, Tang W, Li T. Enhancement of ultrasonically induced cytotoxic effect by hematoporphyrin in vitro. Chemotherapy 2008a;54:364–371.
Wang X, Leung AW, Jiang Y, Yu H, Li X, Xu C. Hypocrellin B-mediated sonodynamic action induces apoptosis of hepatocellular carcinoma cells. Ultrasonics 2012b;52:543–546.
Wang X, Leung AW, Luo J, Xu C. TEM observation of ultrasound-induced mitophagy in nasopharyngeal carcinoma cells in the presence of curcumin. Exp Ther Med 2012c;3:146–148.
Wang X, Liu Q, Wang Z, Wang P, Zhao P, Zhao X, Yang L, Li Y. Role of autophagy in sonodynamic therapy-induced cytotoxicity in S180 cells. Ultrasound Med Biol 2010;36:1933–1946.
Wang X, Wang Y, Wang P, Cheng X, Liu Q. Sonodynamically induced anti-tumor effect with protoporphyrin IX on hepatoma-22 solid tumor. Ultrasonics 2011a;51:539–546.
Wang X, Xia X, Leung AW, Xiang J, Jiang Y, Wang P, Xu J, Yu H, Bai D, Xu C. Ultrasound induces cellular destruction of nasopharyngeal carcinoma cells in the presence of curcumin. Ultrasonics 2011b; 51:165–170.
Wang X, Xia X, Xu C, Xu J, Wang P, Xiang J, Bai D, Leung AW. Ultrasound-induced cell death of nasopharyngeal carcinoma cells in the presence of curcumin. Integr Cancer Ther 2011c;10:70–76.
Wang X, Wang P, Zhang K, Su X, Hou J, Liu Q. Initiation of autophagy and apoptosis by sonodynamic therapy in murine leukemia L1210 cells. Toxicol In Vitro 2013c;27:1247–1259.
Wang XB, Liu QH, Wang P, Tang W, Hao Q. Study of cell killing effect on S180 by ultrasound activating protoporphyrin IX. Ultrasonics 2008b;48:135–140.
Wang XB, Liu QH, Wang P, Zhang K, Tang W, Wang BL. Enhancement of apoptosis by sonodynamic therapy with protoporphyrin IX in isolate sarcoma 180 cells. Cancer Biother Radiopharm 2008c;23: 238–246.
Watanabe Y, Aoi A, Horie S, Tomita N, Mori S, Morikawa H, Matsumura Y, Vassaux G, Kodama T. Low-intensity ultrasound and microbubbles enhance the antitumor effect of cisplatin. Cancer Sci 2008;99:2525–2531.
Wei KC, Chu PC, Wang HY, Huang CY, Chen PY, Tsai HC, Lu YJ, Lee PY, Tseng IC, Feng LY, Hsu PW, Yen TC, Liu HL. Focused ultrasound-induced blood–brain barrier opening to enhance temozolomide delivery for glioblastoma treatment: A preclinical study. PLoS One 2013;8:e58995.
Wood AK, Ansaloni S, Ziemer LS, Lee WM, Feldman MD, Sehgal CM. The antivascular action of physiotherapy ultrasound on murine tumors. Ultrasound Med Biol 2005;31:1403–1410.
Wood AK, Bunte RM, Ansaloni S, Lee WM, Sehgal CM. The antivascular actions of mild intensity ultrasound on a murine neoplasm. In: Clement GT, McDannold NJ, Hynynen K, (eds). Therapeutic ultrasound: 5th International Symposium on Therapeutic Ultrasound. New York: American Institute of Physics; 2006. p. 467–470.
Wood AK, Bunte RM, Cohen JD, Tsai JH, Lee WM, Sehgal CM. The antivascular action of physiotherapy ultrasound on a murine tumor: Role of a microbubble contrast agent. Ultrasound Med Biol 2007;33: 1901–1910.
Wood AK, Bunte RM, Price HE, Deitz MS, Tsai JH, Lee WM, Sehgal CM. The disruption of murine tumor neovasculature by low-intensity ultrasound-comparison between 1- and 3-MHz sonication frequencies. Acad Radiol 2008;15:1133–1141.
Wood AK, Bunte RM, Schultz SM, Sehgal CM. Acute increases in murine tumor echogenicity after antivascular ultrasound therapy: A pilot preclinical study. J Ultrasound Med 2009;28:795–800.
Wood AK, Schultz SM, Lee WM, Bunte RM, Sehgal CM. Antivascular ultrasound therapy extends survival of mice with implanted melanomas. Ultrasound Med Biol 2010;36:853–857.
Wu F, Chen WZ, Bai J, Zou JZ, Wang ZL, Zhu H, Wang ZB. Pathologic changes in human malignant carcinoma treated with high intensity focused ultrasound. Ultrasound Med Biol 2001;27:1099–1106.
Wu F, Chen WZ, Bai J, Zou JZ, Wang ZL, Zhu H, Wang ZB. Tumor vessel disruption resulting from high-intensity focused ultrasound in patients with solid malignancies. Ultrasound Med Biol 2002;28: 535–542.
Xiang J, Xia X, Jiang Y, Leung AW, Wang X, Xu J, Wang P, Yu H, Bai D, Xu C. Apoptosis of ovarian cancer cells induced by methylene blue-mediated sonodynamic action. Ultrasonics 2011;51:390–395.
Xu ZY, Li XQ, Chen S, Cheng Y, Deng JM, Wang ZG. Glioma stem-like cells are less susceptible than glioma cells to sonodynamic therapy with photofrin. Technol Cancer Res Treat 2012;11:615–623.
Xu ZY, Wang K, Li XQ, Chen S, Deng JM, Cheng Y, Wang ZG. The ABCG2 transporter is a key molecular determinant of the efficacy of sonodynamic therapy with photofrin in glioma stem-like cells. Ultrasonics 2013;53:232–238.
Yamaguchi K, Feril LB Jr, Tachibana K, Takahashi A, Matsuo M, Endo H, Harada Y, Nakayama J. Ultrasound-mediated interferon β gene transfection inhibits growth of malignant melanoma. Biochem Biophys Res Commun 2011a;411:137–142.
Yamaguchi S, Kobayashi H, Narita T, Kanehira K, Sonezaki S, Kudo N, Kubota Y, Terasaka S, Houkin K. Sonodynamic therapy using water-dispersed TiO_2–polyethylene glycol compound on glioma cells: Comparison of cytotoxic mechanism with photodynamic therapy. Ultrason Sonochem 2011b;18:1197–1204.
Yan F, Li L, Deng Z, Jin Q, Chen J, Yang W, Yeh CK, Wu J, Shandas R, Liu X, Zheng H. Paclitaxel–liposome-microbubble complexes as ultrasound-triggered therapeutic drug delivery carriers. J Control Release 2013;166:246–255.
Yan F, Li X, Jin Q, Jiang C, Zhang Z, Ling T, Qiu B, Zheng H. Therapeutic ultrasonic microbubbles carrying paclitaxel and LyP-1 peptide: Preparation, characterization and application to ultrasound-assisted chemotherapy in breast cancer cells. Ultrasound Med Biol 2011;37:768–779.
Yanagisawa K, Moriyasu F, Miyahara T, Yuki M, Iijima H. Phagocytosis of ultrasound contrast agent microbubbles by Kupffer cells. Ultrasound Med Biol 2007;33:318–325.
Yang S, Wang P, Wang X, Su X, Liu Q. Activation of microbubbles by low-level therapeutic ultrasound enhances the antitumor effects of doxorubicin. Eur Radiol 2014;24:2739–2753.
Yoshida T, Kondo T, Ogawa R, Feril LB Jr, Zhao QL, Watanabe A, Tsukada K. Combination of doxorubicin and low-intensity ultrasound causes a synergistic enhancement in cell killing and an additive enhancement in apoptosis induction in human lymphoma U937 cells. Cancer Chemother Pharmacol 2008;61:559–567.
Yu T, Bai J, Hu K, Wang Z. Biological effects of ultrasound exposure on adriamycin-resistant and cisplatin-resistant human ovarian carcinoma cell lines in vitro. Ultrason Sonochem 2004a;11:89–94.
Yu T, Huang X, Hu K, Bai J, Wang Z. Treatment of transplanted adriamycin-resistant ovarian cancers in mice by combination of adriamycin and ultrasound exposure. Ultrason Sonochem 2004b; 11:287–291.
Yu T, Wang Z, Mason TJ. A review of research into the uses of low level ultrasound in cancer therapy. Ultrason Sonochem 2004c;11: 95–103.
Yu BF, Wu J, Zhang Y, Sung HW, Xie J, Li RK. Ultrasound-targeted HSVtk and Timp3 gene delivery for synergistically enhanced anti-tumor effects in hepatoma. Cancer Gene Ther 2013;20:290–297.
Yumita N, Iwase Y, Imaizumi T, Sakurazawa A, Kaya Y, Nishi K, Ikeda T, Umemura S, Chen FS, Momose Y. Sonodynamically-induced anticancer effects by functionalized fullerenes. Anticancer Res 2013;33:3145–3151.

Yumita N, Iwase Y, Nishi K, Ikeda T, Komatsu H, Fukai T, Onodera K, Nishi H, Takeda K, Umemura S, Okudaira K, Momose Y. Sonodynamically-induced antitumor effect of mono-l-aspartyl chlorin e6 (NPe6). Anticancer Res 2011;31:501–506.

Yumita N, Iwase Y, Nishi K, Ikeda T, Umemura S, Sakata I, Momose Y. Sonodynamically induced cell damage and membrane lipid peroxidation by novel porphyrin derivative, DCPH–P–Na(I). Anticancer Res 2010;30:2241–2246.

Yumita N, Nishigaki R, Sakata I, Nakajima S, Umemura S. Sonodynamically induced antitumor effect of 4-formyloximethylidene-3-hydroxy-2-vinyl-deuterio-porphynyl(IX)-6,7-dia spartic acid (ATX-S10). Jpn J Cancer Res 2000a;91:255–260.

Yumita N, Nishigaki R, Umemura S. Sonodynamically induced antitumor effect of photofrin II on colon 26 carcinoma. J Cancer Res Clin Oncol 2000b;126:601–606.

Yumita N, Nishigaki R, Umemura K, Umemura S. Hematoporphyrin as a sensitizer of cell-damaging effect of ultrasound. Jpn J Cancer Res 1989;80:219–222.

Yumita N, Nishigaki R, Umemura K, Umemura S. Synergistic effect of ultrasound and hematoporphyrin on sarcoma 180. Jpn J Cancer Res 1990;81:304–308.

Yumita N, Umemura S, Nishigaki R. Ultrasonically induced cell damage enhanced by photofrin II: Mechanism of sonodynamic activation. In Vivo 2000c;14:425–429.

Zhang C, Huang P, Zhang Y, Chen J, Shentu W, Sun Y, Yang Z, Chen S. Anti-tumor efficacy of ultrasonic cavitation is potentiated by concurrent delivery of anti-angiogenic drug in colon cancer. Cancer Lett 2014;347:105–113.

Zhang X, Li K, Cui X, Hu L, Chen Y. Combined pluronic P85- and ultrasound contrast agents-mediated gene transfection to HepG2 cells. J Huazhong Univ Sci Technol Med Sci 2011; 31:842–845.

Zhao YZ, Dai DD, Lu CT, Lv HF, Zhang Y, Li X, Li WF, Wu Y, Jiang L, Li XK, Huang PT, Chen LJ, Lin M. Using acoustic cavitation to enhance chemotherapy of DOX liposomes: Experiment in vitro and in vivo. Drug Dev Ind Pharm 2012;38:1090–1098.

Zhao YZ, Du LN, Lu CT, Jin YG, Ge SP. Potential and problems in ultrasound-responsive drug delivery systems. Int J Nanomed 2013; 8:1621–1633.

Zhao X, Liu Q, Tang W, Wang X, Wang P, Gong L, Wang Y. Damage effects of protoporphyrin IX–sonodynamic therapy on the cytoskeletal F-actin of Ehrlich ascites carcinoma cells. Ultrason Sonochem 2009;16:50–56.

Zheng Y, Zhang Y, Ao M, Zhang P, Zhang H, Li P, Qing L, Wang Z, Ran H. Hematoporphyrin encapsulated PLGA microbubble for contrast enhanced ultrasound imaging and sonodynamic therapy. J Microencapsul 2012;29:437–444.

Zhong H, Li R, Hao YX, Guo YL, Hua X, Zhang XH, Chen ZH. Inhibition effects of high mechanical index ultrasound contrast on hepatic metastasis of cancer in a rat model. Acad Radiol 2010;17: 1345–1349.

Zhou S, Li S, Liu Z, Tang Y, Wang Z, Gong J, Liu C. Ultrasound-targeted microbubble destruction mediated herpes simplex virus-thymidine kinase gene treats hepatoma in mice. J Exp Clin Cancer Res 2010;29:170.

Zolochevska O, Xia X, Williams BJ, Ramsay A, Li S, Figueiredo ML. Sonoporation delivery of interleukin-27 gene therapy efficiently reduces prostate tumor cell growth in vivo. Hum Gene Ther 2011;22: 1537–1550.